Skeletal muscle effects of antisense oligonucleotides targeting glycogen synthase 1 in a mouse model of Pompe disease

Lan Weiss[1*], Michele Carrer[2*], Alyaa Shmara[1], Cheng Cheng[1], Hong Yin[3], Lac Ta[1], Victoria Boock[1], Yasamin Fazeli[1], Mindy Chang[1], Marvin Paguio[1], Jonathan Lee[1], Howard Yu[1], Angela Martin[1], Nina Raben[4], John Weiss[3], Tamar Grossman[2†], Paymaan Jafar-nejad[2], Virginia Kimonis[1#]

Affiliations:

[1] Division of Genetics and Genomic Medicine, Department of Pediatrics, University of California, Irvine, CA 92868, USA

[2] Ionis Pharmaceuticals, Inc., Carlsbad, CA, 92010, USA

[3] Department of Neurology, University of California, Irvine, CA, 92868, USA

[4] Cell and Developmental Biology Center, National Heart, Lung, and Blood Institute, National Institutes of Health, Bethesda, MD, 20892, USA. Current address: M6P Therapeutics, St. Louis, MO

[†] Current address: The Janssen Pharmaceutical Companies of Johnson & Johnson, San Diego, CA, 92121, USA

* These authors contributed equally to this work

[#] To whom correspondence should be addressed:

Virginia Kimonis, MD

Division of Genetics and Genomic Medicine

Department of Pediatrics, Neurology and Pathology

University of California, Irvine

Tel: (949) 824-0571

24 Fax: (949) 824-0171

25 Email: vkimonis@uci.edu

26

27 Abstract words: 2549

28 Manuscript words (excluding abstract): 6176

29 Title characters including spaces:117

30 Number of References:52

31 Number of Tables: 2 supplementary tables

32 Number of figures: 6 main figures and 3 supplementary figures

33

34 **List of abbreviations:**

35 ASO: antisense oligonucleotide; GYS1: glycogen synthase 1; GAA: glucosidase, alpha acid;
36 rhGAA: recombinant human GAA; SRT: substrate reduction therapy; ERT: enzyme replacement
37 therapy; PD: Pompe disease

38

39 **Financial disclosures:**

40 Lan Weiss, Cheng Cheng, Hong Yin, Lac Ta, Victoria Boock, Yasamin Fazeli, Mindy Chang,
41 Marvin Paguio, Jonathan Lee, and Howard Yu report no disclosures. Nina Raben reports no
42 disclosures. Virginia Kimonis is the Principal Investigator for the Rare Diseases Sanofi Registry
43 and has received funding for an investigator initiated and outreach education programs for
44 lysosomal storage diseases. Alyaa Shmara and Angela Martin have received fellowship funding
45 from Sanofi-Genzyme. Michele Carrer, Paymaan Jafar-nejad, and Tamar Grossman are current
46 or former paid employees of Ionis Pharmaceuticals.

ACKNOWLEDGEMENTS

We thank the NIH/NIAMS R21 AR080972-01) (PI Kimonis), Helen Walker Award, AMDA (Acid Maltase Deficiency Association), and the Council on Research, Computing, and Libraries (CORCL), UC Irvine, for funding this study. We thank Jillian Vu, Marvan Youssef and the UCI ULAR staff for their assistance with the animal experiments. We also thank Tracy Reigle and Raul Alonzo (Ionis Pharmaceuticals) for assistance with the preparation of figures.

ABSTRACT

Pompe disease (PD) is a progressive myopathy caused by the aberrant accumulation of glycogen in skeletal and cardiac muscle resulting from the deficiency of the enzyme acid alpha-glucosidase (GAA). Administration of recombinant human GAA as enzyme replacement therapy (ERT) works well in alleviating the cardiac manifestations of PD but loses sustained benefit in ameliorating the skeletal muscle pathology. The limited efficacy of ERT in skeletal muscle is partially attributable to its inability to curb the accumulation of new glycogen produced by the muscle enzyme glycogen synthase 1 (GYS1). Substrate reduction therapies aimed at knocking down GYS1 expression represent a promising avenue to improve Pompe myopathy. However, finding specific inhibitors for GYS1 is challenging given the presence of the highly homologous GYS2 in the liver. Antisense oligonucleotides (ASOs) are chemically modified oligomers that hybridize to their complementary target RNA to induce their degradation with exquisite specificity. In the present study, we show that ASO-mediated Gys1 knockdown in the $Gaa^{-/-}$ mouse model of PD led to a robust reduction in glycogen accumulation in skeletal and cardiac muscle. In addition, combining Gys1 ASO with ERT further reduced glycogen content in muscle, eliminated autophagic buildup and lysosomal dysfunction, and improved motor function in $Gaa^{-/-}$ mice. Our results provide a strong foundation for further validation of the use of Gys1 ASO, alone or in combination with ERT, as a therapy for PD. We propose that early administration of Gys1 ASO in combination with ERT may be the key to preventative treatment options in PD.

76 **INTRODUCTION**

77 Glycogen storage disease type II, also called Pompe disease (PD) is an autosomal recessive
78 disorder affecting between 1 in 17,000 and 1 in 40,000 individuals[1]. PD is caused by the excessive
79 accumulation of glycogen in tissues resulting from inactivating mutations in the GAA gene, which
80 encodes acid alpha-glucosidase, an enzyme responsible for the lysosomal degradation of glycogen.
81 The pathological accumulation of glycogen affects many tissues, but it is by far most impactful in
82 the heart and skeletal muscle of Pompe patients. Indeed, the lack of GAA enzyme activity, or
83 extremely low levels (1–2% of normal), are associated with a fatal infantile cardiomyopathy,
84 profound weakness, and skeletal muscle pathology, whereas 10-20% of normal GAA levels lead
85 to skeletal myopathy with childhood or adult onset[2,3]. To understand the role of GAA in Pompe
86 disease etiology, a mouse model has been generated by targeted deletion of the murine Gaa gene.
87 The Gaa knockout ($Gaa^{-/-}$) mouse recapitulates Pompe disease manifestations, including the
88 accumulation of glycogen in skeletal and cardiac muscle, the autophagy defects, and the
89 consequent myopathy[4].

90 The standard of care for Pompe patients is enzyme replacement therapy (ERT) using recombinant
91 human (rh) GAA (Lumizyme®, or Myozyme®, Sanofi Aventis US LCC), which became
92 commercially available in 2006. ERT has shown positive results in improving the myopathy and
93 cardiomyopathy associated with PD, and therefore has been used to help stabilize or partially
94 improve patient outcomes[5-7]. However, ERT has limited efficacy in the skeletal muscle, as many
95 patients continue to develop progressive muscle weakness despite receiving rhGAA enzyme[8-10].
96 Multiple factors contribute to the poor efficacy of ERT in the skeletal muscle of Pompe patients,
97 particularly when significant disease pathology is present. Some of the limitations affecting ERT
98 are associated with the complexity of delivering a relatively large protein to the muscle tissue.

99 Indeed, when administered via intravenous infusion, the recombinant GAA enzyme circulates to
100 the liver, which acts as a major "sink" and precludes more than 80% of the administered protein
101 from reaching the skeletal muscle[11]. Furthermore, ERT relies on the cation-independent mannose-
102 6-phosphate receptor (CI-MPR), which is expressed at low levels on the membrane of skeletal
103 muscle cells[7]. In addition, dysregulation of autophagy, and the consequent impairment of the
104 autophagosome-lysosome fusion in Pompe myofibers, further contribute to the reduced efficacy
105 of ERT. Ultimately, the failure of autophagy leads to inefficient trafficking of the therapeutic
106 enzyme to the lysosome, limiting its ability to clear the glycogen[12]. This phenomenon is especially
107 evident in type II muscle fibers, which are particularly refractory to ERT[10]. Previous studies
108 performed in mice found upregulated protein levels of enzymes involved in glucose uptake and
109 cytoplasmic glycogen synthesis in skeletal muscle from mice with Pompe disease, including
110 glycogenin (GYG1), glycogen synthase (GYS1), glucose transporter 4 (GLUT4), glycogen
111 branching enzyme 1 (GBE1), and UDP-glucose pyrophosphorylase (UGP2) suggesting a positive
112 feedforward loop for cellular glycogen accumulation[13]. Administration of rhGAA to the Pompe
113 mice normalized not only muscle glycogen levels but also G6P, hexokinase, GS, and glycogenin
114 levels[14]. Thus, it would appear that correction of one aspect of the glycogen metabolic pathway
115 (lysosomal glycogen) results in the correction of multiple other components. Studies in patient
116 biopsies however found that extralysosomal glycogen accumulation in muscle biopsies from late-
117 onset patients was not cleared by ERT, indicating the importance of an acidic pH environment[15].

118 Glycogen synthase (GYS) enzymes catalyze the addition of glucose residues to the growing
119 glycogen molecules by formation of α-1,4-glucosidic linkages. Two paralogous GYS genes, GYS1
120 and GYS2, exist in mice and humans. GYS2 expression is restricted to the liver, where it plays an
121 essential role in the maintenance of proper body glucose homeostasis[16]. GYS1 has a broader

122 expression profile, but it is particularly abundant in skeletal muscle and heart[16]. Decreasing GYS1
123 expression represents a potential therapeutic approach for PD, based on the principle of substrate
124 reduction. Indeed, limiting the synthesis of new glycogen would result in attenuated glycogen
125 accumulation in the muscle tissue. Genetic ablation of murine Gys1 provided proof of principle
126 validation for substrate reduction therapy (SRT) in vivo. Knocking down Gys1 led to restoration
127 of muscle functionality in the $Gaa^{-/-}$ mouse model[17]. Similarly, intramuscular injection of
128 recombinant adeno-associated virus-1 (AAV-1) vector expressing short hairpin ribonucleic acid
129 (shRNA) targeted to Gys1 has been shown to reduce glycogen accumulation in the gastrocnemius
130 of newborn $Gaa^{-/-}$ mice [18]. Altogether the preclinical evidence suggests that reducing GYS1 can be
131 a potential therapeutic approach in Pompe disease, either alone or in combination with ERT.
132 However, GYS1 and GYS2 show high degree of homology, which poses a complex challenge in
133 the identification of safe, isoform-specific inhibitors[19]. It is important to note that no approved
134 small molecule inhibitor is clinically available for the treatment of Pompe disease.

135 Antisense oligonucleotides (ASOs) are short synthetic nucleic acids that hybridize to
136 complementary target RNAs in a sequence-specific manner using Watson-Crick base pairing. By
137 doing so, ASOs can influence RNA processing and regulate protein expression via multiple
138 mechanisms, including RNase H1-mediated mRNA degradation, and splicing modulation[20-24].
139 Over the past two decades ASOs have emerged as both powerful research tools and therapeutic
140 molecules[25-29]. The intrinsic properties of ASOs make them the ideal pharmacological tool to
141 reduce muscle GYS1 expression with exquisite specificity.

142 Here, we show that systemic treatment with a phosphorothioate (PS) 2'-constrained ethyl (cEt)-
143 modified gapmer ASO targeting murine Gys1 not only reversed the excessive glycogen
144 accumulation, but also corrected the autophagic defects present in the skeletal muscle of $Gaa^{-/-}$

145 mice. The ASO-mediated reduction of GYS1 protein, especially when combined with ERT, led to
146 restoration of muscle function in Pompe mice, thus underscoring the in vivo potential of our
147 approach.
148
149 **RESULTS**
150 **Progressive glycogen accumulation and muscle weakness in the Gaa$^{-/-}$ mouse model**
151 We utilized the Gaa knockout mouse model to study the effects of lowering Gys1 expression on
152 Pompe myopathy in vivo. The Gaa$^{-/-}$ mouse was generated and studied by Raben et al. (1998)[4]. To
153 inform the design of appropriate prevention and reversal treatment paradigms, we characterized
154 the progressive accumulation of glycogen in the skeletal and cardiac muscle of the Gaa$^{-/-}$ mice
155 from our colony. We utilized two methods to measure glycogen content in the tissues: a
156 colorimetric biochemical assay, and periodic acid-Schiff (PAS) histochemical staining[4]. As
157 expected, we observed higher amounts of glycogen in the skeletal muscle of Gaa$^{-/-}$ mice compared
158 to wild type mice (Figure 1A). Remarkably, the glycogen levels in quadriceps muscle were already
159 elevated in one-month-old Gaa$^{-/-}$ mice, suggesting that the mutant mice start to accumulate
160 glycogen in skeletal muscle at an early age.

161 The accumulation of glycogen increased progressively over time, from 0.26, to 0.41, and 0.55 µg
162 glycogen per µg of total protein in quadriceps muscle homogenate from one-, two-, and three-
163 month-old Gaa$^{-/-}$ mice, respectively (Figure 1A). Similar to previous reports [4,30,31], the excessive
164 glycogen accumulation in the skeletal muscle was associated with a progressive decline in motor
165 function in aging Gaa$^{-/-}$ mice, as assessed by the rotarod test (Figure 1B).
166
167 **Different levels of ASO-mediated Gys1 knockdown lead to the proportional amelioration of**

168 **aberrant glycogen accumulation in the skeletal muscle of young Gaa$^{-/-}$ mice**

169 Through in vitro and in vivo screening, we identified two ASOs targeting mouse Gys1 that were
170 potent and well tolerated in mice (Supplementary Figure 1, 2). When dosed systemically to wild
171 type mice via subcutaneous injection for six weeks, Gys1 ASO#1 and ASO#2 resulted in the
172 efficient, dose-dependent knockdown of murine Gys1 mRNA. ASO#1 had an ED_{50} of 45.2 mg/kg
173 (95% confidence interval (C.I.): 32.3-63.2 mg/kg) in quadriceps muscle, whereas ASO#2 was
174 more potent, with an ED_{50} of 24.2 mg/kg (95% C.I.: 22.4-26.1 mg/kg) (Supplementary Figure 1A).
175 Consistently, Gys1 ASO#2 achieved a robust reduction of GYS1 protein in skeletal muscle of wild
176 type and Gaa$^{-/-}$ mice (Supplementary Figure 1B, 1C).

177 To determine if ASO-mediated Gys1 knockdown attenuates the pathological accumulation of
178 glycogen in vivo, we dosed young Gaa$^{-/-}$ mice with the newly identified Gys1 ASO#1 and ASO#2.
179 A starting age of one month was selected because at this time the Gaa$^{-/-}$ mice have not developed
180 severe myopathy, yet, and the glycogen is only starting to accumulate in the skeletal muscle
181 (Figure 1A). The one-month-old Gaa$^{-/-}$ mice (Cohort 1) were dosed via subcutaneous injection with
182 25 mg/kg Gys1 or control ASO, once a week for sixteen weeks (Figure 2A). Compared to control
183 ASO, Gys1 ASO#1 and ASO#2 resulted in 83.64% (95% C.I.: 77.40-88.58) and 88.58% (95%
184 C.I.: 83.61-92.06) Gys1 mRNA knockdown, respectively in quadriceps muscle (Figure 2B,
185 Supplementary Table 1). Corroborating the reduction in mRNA expression, compared to control
186 ASO, ASO#2 administration decreased GYS1 protein, measured by Western blot, in key Pompe
187 tissues of Gaa$^{-/-}$ mice by 100%, 98%, and 100% in quadriceps, diaphragm, and heart, respectively.
188 (Figure 2C, Supplementary Table 1).

189 To evaluate the impact of Gys1 knockdown on excessive glycogen accumulation in the muscle of
190 the Pompe mice, we measured glycogen content by a colorimetric biochemical assay in the muscle

191 of the 20-week-old Gaa$^{-/-}$ mice following 16 weeks of Gys1 ASO treatment. ASO#1 resulted in a
192 38.06% reduction in glycogen content (0.29 μg/μg protein) in quadriceps muscle, and ASO#2
193 resulted in 57.05% reduction in glycogen (0.19 μg/μg protein) compared to control ASO (0.49
194 μg/μg protein) (Figure 2D, Supplementary Table 1). The superior efficacy of ASO#2 compared to
195 ASO#1 is consistent with its greater potency in knocking down Gys1 mRNA expression. Similarly,
196 the control ASO had no effect on Gys1 expression and glycogen content (Figure 2B-E). In
197 agreement with the biochemical measurements, semi-quantitative analysis of glycogen content in
198 histological sections using PAS staining confirmed that Gys1 ASOs ameliorated the aberrant
199 accumulation of glycogen in Gaa$^{-/-}$ quadriceps muscle. On a scale of 1 (no staining) to 4 (extensive
200 staining), an average score of 1.8 was assigned to the 4.5-month-old Gaa$^{-/-}$ mice treated with
201 control ASO, 1.4 to mice treated with ASO#1, and 1 to mice treated with ASO#2 (Figure 2E,
202 Supplementary Table 2).

203 In view of the enhanced efficacy in the early-treatment setting, we selected ASO#2 to further
204 investigate if Gys1 ASO treatment could revert the Pompe pathology in older Gaa$^{-/-}$ mice.

205

206 **ASO-mediated Gys1 reduction partially reverses glycogen accumulation in skeletal muscle**
207 **of older Gaa$^{-/-}$ mice**

208 To assess if therapeutic treatment with Gys1 ASO could reverse the glycogen accumulation and
209 myopathy in mature Pompe mice, we dosed older Gaa$^{-/-}$ mice with Gys1 ASO#2 starting at three
210 months of age (Cohort 2) (Figure 3A). Gys1 ASO#2 was administered by weekly subcutaneous
211 injections at 25 mg/kg for 16 weeks (Figure 3A). The rotarod motor performance assay showed
212 that the ASO#2-mediated knockdown of Gys1 expression resulted in a trend towards preservation
213 of motor function (Figure 3B), which otherwise progressively declines in Gaa$^{-/-}$ mice (Figure 1B,

214 3B). Indeed, the control ASO did not slow down the deterioration of muscle function in Pompe
215 mice (Figure 3B). We sacrificed the animals at 6.5 months of age and studied the quadriceps
216 muscle, diaphragm, and heart tissue from mice treated with Gys1 ASO#2. We measured a 64.71%
217 (95% C.I.: 57.00-71.05) knockdown of mouse Gys1 mRNA and complete depletion of GYS1
218 protein in quadriceps muscle compared to control ASO (Figure 3C-D, Supplementary Table 1).
219 Similarly, GYS1 protein was reduced by 80% in diaphragm and 70% in heart compared to mice
220 treated with control ASO (Figure 3D, Supplementary Table 1). Of note, the expression of GYS1
221 was not significantly different in 6.5-month-old Pompe mice compared to wild type mice (Figure
222 3D). A biochemical assay demonstrated that the ASO#2-mediated knockdown of Gys1 expression
223 was associated with a modest 7.79% (95% C.I.: 5.53-28.45) reduction in glycogen accumulation
224 compared to control ASO in the quadriceps muscle of $Gaa^{-/-}$ mice (Figure 3E, Supplementary Table
225 1). In addition, semi-quantitative analysis of histological sections of quadriceps muscle using PAS
226 staining confirmed a mild improvement of the aberrant glycogen accumulation following treatment
227 with Gys1 ASO#2 (average score of 1.25 on a scale of 1 to 4) compared to control ASO (average
228 score of 2.2) (Figure 3F, Supplementary Table 2).

229

230 **ASO mediated Gys1 knockdown in combination with enzyme replacement therapy further**
231 **reverses Pompe pathology, preserving motor function in older $Gaa^{-/-}$ mice**

232 Substrate reduction therapy (SRT) using ASO to remove the source of new glycogen synthetized
233 via GYS1 shows promise as a monotherapy, but the reversal of the myopathy in $Gaa^{-/-}$ mice was
234 incomplete in 6.5-month-old animals. We reasoned that combining Gys1 ASO, which blocks the
235 synthesis of new glycogen, with GAA enzyme replacement therapy (ERT) to simultaneously
236 remove pre-existing glycogen in the skeletal muscle and heart of older Pompe mice, could provide

237 additive efficacy. Therefore, we dosed four-month-old Gaa$^{-/-}$ mice with Gys1 ASO#2 at 25 mg/kg
238 by weekly subcutaneous injections for six weeks, followed by a 10-week-long co-administration
239 phase where we combined ASO#2 and ERT, in the form of recombinant human alpha-acid
240 glucosidase (rhGAA) enzyme (Cohort 3) (Figure 4A). rhGAA was dosed intravenously every two
241 weeks (Figure 4A). Alternatively, Gaa$^{-/-}$ mice were dosed with either ASO#2 alone or ERT alone
242 (Figure 4A). Wild type mice and PBS-treated Gaa$^{-/-}$ mice were included in the study as controls.
243 The ASO#2+ERT combination treatment led to a stable increase in rotarod performance over the
244 4-month-long treatment, resulting in gains of 9, 8, 11 and 19% compared to baseline after 1, 2, 3,
245 and 4 months of treatment, respectively. On the other hand, ASO#2 alone increased the rotarod
246 performance in the first three months of treatment, but was followed by a slowdown (2, 10, 12 and
247 7% gain compared to baseline after 1, 2, 3, and 4 months of treatment, respectively). ERT alone
248 was unable to prevent the functional decline in the aging Pompe mice, resulting in a downward
249 change in rotarod performance over time (-2, -8, -5 and -8% compared to baseline after 1, 2, 3, and
250 4 months of treatment, respectively) (Figure 4B).

251 At the end of the study, the 8-month-old mice were sacrificed for further biochemical and IHC
252 analysis of the muscle tissue. Western blot analysis revealed that ASO#2 alone or ASO#2+ERT
253 resulted in the complete ablation of GYS1 protein expression in quadriceps muscle and heart
254 (Figure 4C). Similarly, minimal residual GYS1 protein was present in the diaphragm of the same
255 treatment groups (Figure 4C). On the other hand, Gaa$^{-/-}$ mice that received PBS or ERT alone had
256 robust GYS1 protein expression, comparable to wild type levels (Figure 4C). Importantly, the
257 systemic administration of Gys1 ASO#2, alone or in combination with ERT, was well tolerated in
258 Pompe mice with no significant changes in body or organ weights, and no significant elevation in

259 liver transaminases, blood urea nitrogen, or muscle creatine kinase in plasma compared to control
260 groups (Supplementary Figure 2).

261 The average glycogen content measured using the biochemical assay in quadriceps muscle of Gaa^{-}
262 $^{/-}$ mice was 24.85 (95% C.I.: 12.54-37.17), 10.98 (95% C.I.: 6.57-15.38), 4.84 (95% C.I. 1.61-
263 8.07), and 20.5 (95% C.I.: 12.46-28.53) μg glycogen per μg total protein in the PBS, ASO alone,
264 ASO+ERT, and ERT alone treatment groups, respectively (Figure 4D). Therefore, compared to
265 PBS controls, the biochemical glycogen assay revealed a 55.22% (95% C.I.: 20.29-74.84)
266 reduction in glycogen content in quadriceps muscle of Gaa$^{-/-}$ mice dosed with ASO#2 alone (Figure
267 4D, Supplementary Table 1). The ASO#2+ERT combination resulted in an even greater effect,
268 reducing glycogen levels by 83.48% (95% C.I.: 53.80-94.10) in quadriceps muscle (Figure 4D,
269 Supplementary Table 1). ERT alone did not significantly attenuate the glycogen accumulation,
270 leading to 15.78% (95% C.I.: 11.61-31.49) less glycogen in quadriceps muscle of Gaa$^{-/-}$ mice. ERT
271 was more efficacious in the heart, where it resulted in 65.82% (95% C.I.: 5.88-87.59) glycogen
272 reduction vs. PBS control when dosed alone, and in 74.93% (95% C.I.: 18.77-92.26) glycogen
273 reduction vs. PBS control when combined with Gys1 ASO#2 (Figure 4D, Supplementary Table
274 1). PAS staining of quadriceps muscle histological sections corroborated the biochemical assay
275 results, showing a marked reduction in glycogen content, especially in the ASO#2 group (semi-
276 quantitative score of 1.5 on a scale of 1 to 4, where 1 is no glycogen detected) and ASO#2+ERT
277 (score of 1), compared to PBS (score of 3.75) or ERT alone (score of 3) samples (Figure 4E,
278 Supplementary Table 2). Thus, the motor function improvement correlated well with the reduction
279 in muscle glycogen content.

280 Taken together, our data supports the hypothesis that blocking the synthesis of new glycogen while
281 concomitantly enhancing its clearance is beneficial in treating both the skeletal muscle and cardiac
282 abnormalities in Pompe disease (Figure 6).
283

284 **ASO-mediated Gys1 knockdown with or without ERT, but not ERT alone, ameliorates the**
285 **autophagic buildup in the skeletal muscle of Gaa$^{-/-}$ mice**

286 Defective autophagy is a major factor contributing to the muscle pathology in Pompe disease[7].
287 Consistent with the highly integrated functions of lysosomes and autophagosomes, it has been
288 shown that lysosomal dysfunction in Pompe disease leads to a block in autophagic flux and
289 accumulation of autophagic debris, particularly in muscle tissue[32]. It is important to note that the
290 Gaa$^{-/-}$ mouse model faithfully recapitulates the autophagic defects described in Pompe patients[30].
291 Incomplete autophagic flux can be assessed by measuring the aberrant accumulation of LC3 and
292 p62 proteins. Additionally, immunostaining of histological sections for lysosomal-associated
293 membrane protein 1 (LAMP1) provides a method to detect enlarged lysosomes[33,34]. We
294 investigated the efficacy of Gys1 ASO, alone or in combination with ERT (Cohort 3, Figure 4A),
295 in ameliorating the defective autophagy in Gaa$^{-/-}$ mice. Western blot analysis confirmed
296 accumulation of p62 and LC3-II proteins in quadriceps muscle and heart of 8-month-old Gaa$^{-/-}$
297 mice treated with PBS (Figure 5A). ERT alone alleviated the autophagic defect in the heart but not
298 significantly in the skeletal muscle, as indicated by the reduced levels of LC3-II, p62 and LAMP1
299 proteins in cardiac tissue with no major effect in quadriceps muscle (Figure 5A). On the other
300 hand, Gys1 ASO#2, alone or in combination with ERT, led to the almost complete normalization
301 of the p62, LC3-II and LAMP1 protein levels in quadriceps of Gaa$^{-/-}$ mice (Figure 5A). In the
302 heart, the Gys1 ASO contributed to a lesser extent to the reduction of the autophagic markers

303 (Figure 5A). In addition, immunostaining of histological sections confirmed that ASO#2+ERT
304 administration reduced LAMP1 protein levels in quadriceps muscle of Gaa$^{-/-}$ mice (Figure 5A,
305 5B), suggesting that the combination therapy could rescue the autophagy pathway dysfunction in
306 Pompe muscle after four months of treatment. The effect was more pronounced than in the Gys1
307 ASO#2-only group (Figure 5B).

308 In conclusion, our data indicate that the combination of Gys1 ASO and ERT might provide
309 therapeutic benefit by targeting various aspects of Pompe pathogenesis, namely glycogen
310 accumulation and autophagy defects.

311

312 **Systemic Gys1 knockdown does not mitigate Pompe pathology in the central nervous system**

313 Pompe disease is a complex multi-systemic condition with growing evidence of central nervous
314 system (CNS) involvement[35]. Indeed, we found remarkable abnormalities in the spinal cord of
315 Gaa$^{-/-}$ mice at 8 months of age (Supplementary Figure 3). The pathologic changes were visible in
316 histological sections of the spinal cord, where Nissl staining (toluidine blue) revealed the presence
317 of swollen cell bodies, activated glial cells, and centronucleated cells (Supplementary Figure 3).
318 Systemically delivered Gys1 ASO#2 did not ameliorate the Pompe CNS phenotype of Gaa$^{-/-}$ mice
319 (Supplementary Figure 3), consistent with the inability of ASOs to cross the blood-brain barrier.

320

321 **DISCUSSION**

322 Enzyme replacement therapy, currently the standard of care for patients with PD, has been shown
323 to be beneficial, but its efficacy is hindered by some limitations, especially in treating the skeletal
324 muscle manifestations of PD. Early administration of ERT improves cardiac hypertrophy and
325 motor development, extending the chances of survival in patients with infantile-onset disease

326 (IOPD)[6,36]. Patients with the late-onset form (LOPD) have early increase and stabilization of their
327 pulmonary and motor function, however after reaching a plateau there is continued decline in their
328 motor function such as the 6 Minute Walk Test[8,9]. Progressive muscle weakness thus continues to
329 be a problem for long-term survivors of PD[5,6]. An explanation is provided by studies that have
330 shown that the delivery of the therapeutic enzyme to skeletal muscle is insufficient to reduce the
331 glycogen content and eliminate the autophagic buildup[6]. Recently, a study using a new adjunct
332 therapy based on the enzyme and chaperone ATB200/AT222 combination showed enhanced
333 efficacy over the currently approved ERT in Gaa$^{-/-}$ mice. ATB200/AT222 was able to normalize
334 muscle glycogen content and reduced the levels of lysosomal and autophagosomal markers in the
335 muscle of Gaa$^{-/-}$ mice to wild type levels[7,18]. Clinical trials of AT2221/ATB200 have been
336 completed and this approved treatment now offers an alternative effective therapeutic option for
337 Pompe disease patients.

338 Douillard-Guilloux et al. (2008) demonstrated that intramuscular injection of AAV-1 expressing
339 shRNA targeted to Gys1 reduces glycogen accumulation in the gastrocnemius of newborn Gaa$^{-/-}$
340 mice[19]. The same research group also analyzed the effect of a complete genetic ablation of
341 glycogen synthesis in a new Gaa/Gys1 double knock-out (KO) mouse model[17]. The Gaa/Gys1 KO
342 mouse exhibited a profound reduction in cardiac and skeletal muscle glycogen, a significant
343 decrease in lysosomal swelling and autophagic buildup, and complete correction of
344 cardiomegaly[17]. Muscle atrophy, observed in 11-month-old single Gaa KO mice, was less
345 pronounced in the Gaa/Gys1 double KO mice, resulting in improved exercise capacity[17]. This data
346 demonstrated that long-term suppression of muscle glycogen synthesis is well tolerated and leads
347 to a significant improvement in Pompe pathology. However, no approved small molecule

348 inhibitors of muscle GYS1 are currently clinically available, underscoring the challenges of
349 finding specific compounds that can preserve the activity of the hepatic GYS2 enzyme.

350 ASO technology has emerged as a highly specific therapeutic option for a variety of neuromuscular
351 diseases. ASOs that modulate exon splicing of the dystrophin (DMD) gene can reduce muscle
352 degeneration in Duchenne's muscular dystrophy[37-39,11,40,41]. An ASO that disrupts spliceosome
353 action on exon 7 of the survival motor neuron 1 (SMN1) gene and restores the gene to functioning
354 length has been approved for treatment of spinal muscular atrophy[42,43]. Recently, an ASO with
355 RNase H1 mechanism has been approved by the FDA for amyotrophic lateral sclerosis (ALS)
356 patients with SOD1 mutations[41,42]. Several studies have attempted to use ASOs to mitigate the
357 disease outcomes by improving or restoring normal GAA synthesis[6]. Van der Wal et al. (2017)
358 studied the common IVS132-13T>G GAA mutation and located sequences where an ASO could
359 block splicing machinery and prevent exclusion of exon 2 in the final transcript, leading to
360 increased GAA expression[44,45]. Goina et al. (2017) performed a similar exon 2 splicing modulation
361 with an ASO and successfully reduced glycogen accumulation in patient-derived myotubes[46].
362 Other ASO studies have sought to reduce glycogen by interfering with GYS1 expression. Clayton
363 et al. (2014) demonstrated that treating Pompe mice with a phosphorodiamidate morpholino
364 oligonucleotide (PMO) designed to induce exon 6 skipping in the murine Gys1 mRNA resulted in
365 the degradation of messenger RNA due to frame shift[16]. However, to facilitate PMO delivery to
366 muscle via systemic administration, the PMO was conjugated with a cell penetrating peptide (GS-
367 PPMO), and the development of PPMO drugs for human use is significantly challenged by their
368 potential toxicity, as observed in primate studies[46]. This toxicity is likely due to the cationic nature
369 of the peptide at the doses required for efficacious exon skipping in the primate musculature[16,47].
370 Benefiting from advancements in ASO technology, here we identified a potent ASO that safely

371 knocks down mouse Gys1 expression by RNase H1 mechanism in mice. Using both prevention
372 and reversal treatment modalities, we demonstrated the potential of the Gys1 ASO approach to
373 serve as efficacious SRT in the Gaa$^{-/-}$ mouse model of Pompe disease.

374 The Gaa$^{-/-}$ Pompe mice start to accumulate glycogen in skeletal muscle as early as three weeks of
375 age but develop a progressive defect in motor functions from six months of age. We have attempted
376 to address the importance of timing in two separate cohorts, starting the ASO treatment at one-
377 and three-month-old mice respectively. Taken together, our data indicate that long-term
378 elimination of muscle glycogen synthesis leads to a significant reduction of glycogen accumulation
379 and autophagic buildup, as well as a tendency towards functional improvement in severely affected
380 older Pompe mice. Interestingly, we observed superior activity of Gys1 ASO in the skeletal muscle
381 of Pompe mice compared to wild type, healthy mice (Supplementary Figure 1). We hypothesize
382 this phenomenon being the result of increased permeability to ASO of the damaged muscle
383 combined with facilitated escape of the ASO from defective endosomal compartments upon
384 cellular uptake.

385 Despite the positive results obtained by knocking down Gys1 expression with ASO, there was still
386 a residual amount of glycogen present in the skeletal muscle of older Gaa$^{-/-}$ mice, and the muscle
387 structure abnormality was not significantly improved upon treatment with ASO alone
388 (Supplementary Table 2). This could be due to compensatory mechanisms, or very low levels of
389 residual GYS1 enzymatic activity. To further improve the efficacy of our Gys1 ASO-based SRT
390 approach both in the skeletal muscle and heart, we decided to combine the ASO treatment with
391 ERT. Our data shows that the combination of Gys1 ASO with rhGAA results in enhanced
392 reduction of glycogen content and reversal of the autophagy defect in the skeletal muscle of old
393 Gaa$^{-/-}$ mice. The molecular changes induced by the ASO and ERT treatment led to the preservation

394 of motor function in the aging Pompe mice. Recently Ullman et al. (2024)[48] recently reported their
395 preclinical studies of MZ-101, a selective and noncompetitive inhibitor of GYS1, reduced
396 glycogen accumulation, similar to that of ERT alone in Pompe mouse models. MZ-101 when
397 utilized in combination with ERT however had an additive effect of normalizing glycogen
398 concentrations in the muscles. These data from prior studies and our promising data suggests
399 that substrate reduction therapy with GYS1 inhibition may be a promising therapeutic approach
400 for Pompe disease. Recently, Maze Therapeutics announced positive phase 1 study results from a
401 clinical trial of the small molecule GYS1 inhibitor MZE001 (ClinicalTrials.gov Identifier:
402 NCT05249621). In the study the healthy volunteers demonstrated exposure-dependent
403 reductions in blood mononuclear cell glycogen across dose levels 10 days after administration. It
404 is also expected that GYS1 ASOs has the potential to be used as monotherapy or in combination
405 with ERT in future clinical trials in Pompe patients. The results from the clinical trial further
406 support the validity and safety of GYS1 inhibition as a potential therapeutic approach for Pompe
407 disease.
408

409 **MATERIALS AND METHODS**

410 **Identification of antisense oligonucleotides (ASOs) targeting mouse Gys1**

411 All ASOs used in the studies described here were 16 nucleotides in length with a phosphorothioate
412 (PS) backbone and three 2'-constrained ethyl (cEt)-modified nucleotides at both ends (3-10-3
413 gapmer configuration). A well-characterized control ASO which does not hybridize to any mouse
414 mRNA sequence was included in the experiments. The oligonucleotides were synthesized and
415 purified as previously described[49]. ASOs targeting murine Gys1 were designed and initially
416 screened for activity in B16-F10 cells via electroporation. The most active ASOs were

417 subsequently evaluated in wild type mice to identify ASOs that were safe and active in vivo. A
418 dose-response confirmation experiment for the two lead ASOs, ASO#1 and ASO#2, was
419 performed in wild type mice by subcutaneous injection twice a week for 5.5 weeks at 12.5, 25, 50,
420 and 100 mg/kg total weekly doses (shown in Supplementary Figure 1A). All ASOs were
421 formulated in phosphate buffered saline (PBS) and were administered to mice by subcutaneous
422 injection. The mouse ASO screening studies were conducted under protocols approved by the
423 Institutional Animal Care and Use Committees at Ionis Pharmaceuticals.
424

425 **Characterization of the Gaa$^{-/-}$ animal model of Pompe disease**

426 The Gaa$^{-/-}$ Pompe mouse model was a gift of Dr. Nina Raben[50]. The mouse model is a constitutive
427 homozygote knockout of the murine acid alpha-glucosidase (Gaa) gene. One-month-old Gaa$^{-/-}$
428 mice, which show only the initial signs of tissue glycogen accumulation without severe myopathy,
429 were used in prevention studies, whereas three-month-old Gaa$^{-/-}$ mice, which show marked
430 glycogen accumulation and motor function impairment, were used in reversal studies. All the
431 intervention studies performed in either the Gaa$^{-/-}$ mouse model or wild type C57BL/6 control mice
432 were conducted in accordance with the Institutional Animal Care and Use Committee at the
433 University of California, Irvine (UCI), under protocol IACUC AUP-19-075, and were consistent
434 with Federal guidelines. The mice were housed at UCI animal facility that maintained a constant
435 temperature (22°C) and controlled light and dark cycles (12:12). The overall condition of the mice
436 was monitored daily throughout the experimental process to assess general health and mitigate any
437 pain and suffering.
438

439 **Administration of ASOs to Gaa$^{-/-}$ mice**

440 Gaa$^{-/-}$ or wild type control mice were dosed with ASOs once a week at 25 mg/kg via subcutaneous
441 injection. For the early-treatment study (Cohort 1) described in Figure 2, one-month-old Gaa$^{-/-}$
442 mice were randomly divided into groups for treatment with different Gys1 ASOs, control ASO, or
443 vehicle (PBS), n=12-17 mice per group. For the reversal study (Cohort 2) described in Figure 3,
444 three-month-old Gaa$^{-/-}$ mice were randomly divided into three groups for treatment with Gys1
445 ASO#2 (n=15), control ASO (n=10), or vehicle (PBS) (n=10). The mice received a total of 16
446 weekly ASO doses (16 weeks duration) and were sacrificed 48 hours after the last ASO dose. Body
447 weight changes, and the weight of liver, kidney, and spleen were recorded to exclude potential
448 toxicity of the ASOs in the context of the long dosing paradigm in diseased Gaa$^{-/-}$ mice.
449

450 **Adjunct treatment using Gys1 ASO in combination with ERT in Gaa$^{-/-}$ mice**

451 Four-month-old Gaa$^{-/-}$ mice were dosed with Gys1 ASO#2 or control ASO by subcutaneous
452 injection once a week at 25 mg/kg for six weeks. Starting from week 7 the mice additionally
453 received 20 mg/kg recombinant human GAA (rhGAA) (Genzyme Corporation, Cambridge, MA;
454 Cat.: NDC 58468-0160-1) via intravenous injection once every two weeks. The antihistaminic
455 agent diphenhydramine hydrochloride was administered to the mice via intraperitoneal injection
456 15 minutes before receiving the human enzyme, starting from the second rhGAA administration.
457 The weekly subcutaneous ASO administration continued throughout the ERT phase for a total of
458 16 doses. The mice were euthanized at 8 months of age, after having been treated with Gys1 ASO
459 for 4 months, the last two of which overlapped with the ERT; n=5 per treatment group.
460

461 **Accelerating rotarod performance test**

462 Muscle function was evaluated using a rotarod apparatus (Rotamex-5, Columbus Instruments,
463 Columbus, OH). Briefly, mice were placed on a rotarod whose speed was set to progressively
464 increase from 4 to 40 rotations per minute (rpm) in 300 seconds. The latency to fall from the
465 rotating rod was recorded as a measure of muscle strength. Assessments were done on three
466 consecutive days, three to five trials each day with at least two-minute rest intervals between the
467 trials. The mean latency time to fall off the rotarod from three independent trials from the last two
468 days was used for analysis.
469
470 **Biochemical analysis of serum from mice for toxicity studies**
471 Blood samples were collected from mice via cardiac puncture under deep anesthesia using
472 isoflurane inhalation. Immediately after collection, approximately 300-500 µL of whole blood
473 were placed into serum separator tubes (Greiner Bio-One Minicollect tubes; Cat.: 450472).
474 Samples were allowed to clot for at least 20 minutes at room temperature, and then centrifuged at
475 3,000 rpm for 15 minutes. Serum was transferred to fresh tubes and stored at -80ºC before being
476 used for clinical biochemistry evaluation at IDEXX Laboratories (IDEXX Laboratories Inc.,
477 Maine, USA). Parameters measured include alanine aminotransferase, aspartate aminotransferase,
478 alkaline phosphatase, blood urea nitrogen, creatine kinase.
479
480 **Gene expression analysis using quantitative real-time PCR**
481 Tissue samples were isolated from mice and snap frozen in liquid nitrogen. Frozen tissues were
482 homogenized in TRIzol reagent (Thermo Scientific, Waltham, MA; Cat.: 15596026), and total
483 RNA was extracted according to the manufacturer's instructions. Real-time qPCR analysis was
484 performed using the following reagents: mouse Gys1 (Taqman™ assay ID: Mm01962575_s1),

485 mouse Gapdh (Taqman™ assay ID: Mm 99999915_g1, housekeeping gene). In the initial
486 assessment of ASO activity in wild type mice (Supplementary Figure 1A) real-time qPCR analysis
487 was performed using the following primer-probe sets: mouse Gys1 (forward primer: 5'-
488 TGATGAAGAGAGCCATCTTTGC-3'; reverse primer: 5'-AGGAGTCGTCCAGCATGTTGT-
489 3'; probe: 5'-ACTCAGCGGCAGTCTTTCCCACCA-3'), mouse cyclophilin A (forward primer:
490 5'-TCGCCGCTTGCTGCA-3'; reverse primer: 5'-ATCGGCCGTGATGTCGA-3'; probe: 5'-
491 CCATGGTCAACCCCACCGTGTTC-3'). Reactions were conducted in triplicate on a
492 QuantStudio7 real-time PCR system (Thermo Fisher Scientific, Waltham, MA), following the
493 manufacturer's instructions.
494
495 **Biochemical measurement of tissue glycogen content**
496 Mouse tissues were collected, snap frozen in liquid nitrogen upon collection, and stored at -80ºC.
497 Approximately 10 mg of frozen quadriceps muscle were rinsed in 300 µL of ice-cold PBS, then
498 homogenized in 200 µL of double-distilled water using a Wheaton dounce tissue grinder (DWK
499 Life Sciences, Rockwood, TN) as follows: 10-20 passes on loose pestle followed by 10-20 passes
500 on tight pestle, keeping the tissue grinder on ice. The tissue lysates were then heated at 100°C for
501 10 minutes, then centrifuged at 15,000 g at 4°C for 10 minutes. Total protein concentration in the
502 supernatant was determined using the Micro BCA protein assay kit (Thermo Scientific, Waltham,
503 MA; Cat.: 23235). In the same supernatant, glycogen concentration was measured using a
504 fluorometric enzymatic assay (Sigma-Aldrich, St. Louis, MO; Cat.: MAK016), according to the
505 manufacturer's instructions. The assay produces a fluorometric (λex = 535/λem = 587 nm) product
506 proportional to the glycogen present in the sample. The fluorescent signal was analyzed using the

507 BioTek Gen5 software (Agilent Technologies, La Jolla, CA), and normalized by the total protein
508 content of the sample.
509
510 **Western blot analysis of autophagy markers**
511 Approximately 30 mg of frozen tissue was homogenized in 500 μL of RIPA buffer (Sigma-
512 Aldrich, St. Louis, MO; Cat.: R0278) supplemented with a proteinase inhibitor cocktail (Sigma-
513 Aldrich, St. Louis, MO; Cat.: P8340) using a handheld electric homogenizer (Qsonica, Newtown,
514 CT; Cat.: XL-2000). The tissue homogenate was then agitated on a Benchmark Roto-Mini Plus
515 (Benchmark Scientific, Sayreville, NJ) for 2 hours at 4°C. Lastly, the tissue lysate was centrifuged
516 at 20,000 g at 4°C for 30 minutes, and the supernatant was collected for analysis. The sample
517 protein concentration was measured using the Micro BCA protein assay kit (Thermo Fisher
518 Scientific, Waltham, MA; Cat.: 23235). 20 μg of total protein lysate was resolved by
519 electrophoresis on Bis-Tris 4-12% NuPAGE polyacrylamide gels using the Novex Mini Cell
520 system (Invitrogen/Thermo Fisher Scientific, Waltham, MA). The proteins were then transferred
521 to a PVDF membrane, which was later blocked with 1% bovine serum albumin (BSA) in Tris-
522 buffered saline containing 0.1% Tween 20 (TBS-T). The primary antibodies used in our studies
523 were: anti-GYS1 (Abcam, Waltham, MA; Cat.: ab 40810; 1:5,000 dilution), anti-LC3B-I/II
524 (Abcam, Waltham, MA; Cat.: ab192890 ; 1:5,000 dilution), anti-p62 (Abcam, Waltham, MA; Cat.:
525 ab56416; 1:20,000 dilution), anti-LAMP1 (Abcam, Waltham, MA; Cat.: ab27170; 1:2,000
526 dilution), anti-GAPDH (Abcam, Waltham, MA; Cat.: ab18160; 1:10,000 dilution; served as
527 loading control), anti-β-ACTIN (Abcam, Waltham, MA; Cat.: ab8227; 1:5,000 dilution; served as
528 alternative loading control). Horseradish peroxidase (HRP)-linked goat anti-mouse or goat anti-

529 rabbit secondary antibodies were used (1:5,000 dilution). Densitometric quantification was
530 performed using ImageJ software (National Institutes of Health, Bethesda, MD).
531
532 **Periodic acid-Schiff Histological analysis**
533 Periodic acid-Schiff (PAS) staining was performed to detect glycogen in histological tissue
534 sections. Briefly, the quadriceps muscle was dissected and fixed in a 4% neutral buffered formalin
535 solution at room temperature for 20 hours. The fixed tissue was then rinsed in PBS and transferred
536 to a 70% ethanol solution before being embedded in paraffin blocks and sectioned. The PAS
537 staining was performed on 8μm-thick sections by the Pathology Department at UCI Medical
538 Center according to protocols described previously[49]. Images of the histological slices were
539 captured using a Keyence BZ-810 microscope (Keyence, Itasca, IL). In PAS-stained tissue
540 sections, glycogen appears fuchsia-colored under light microscopy. For quantification of the PAS
541 staining, the histological sections of quadriceps muscle from 4-5 animals per treatment group were
542 analyzed, and a semi-quantitative score from 1 (no staining) to 4 (extensive staining) was assigned
543 to each section. The scoring was performed independently by two different technicians to ensure
544 accurate assessment. To quantify the number of myofibers with centralized nuclei, a minimum of
545 300 myofibers per animal were manually evaluated in the PAS-stained sections of quadriceps
546 muscle (n=4-5 mice per each group). The data is presented as the percentage of myofibers with a
547 centralized nucleus.
548
549 **Immunohistochemistry (IHC) studies**
550 For lysosomal analysis, the expression of lysosomal associated membrane protein 1 (LAMP1)
551 was assessed using IHC in tissue sections of quadriceps muscle embedded in frozen section

552 medium (Fisher Scientific, Hampton, NH; Cat.: 22-046-511), as described previously[51]. Briefly,
553 8µm-thick cryosections (10 sections per each animal, 5 animals per treatment group) were fixed
554 in 4% paraformaldehyde (PFA), blocked in donkey serum, and stained with an anti-LAMP1
555 primary antibody (Abcam, Waltham, MA; Cat.: ab24170; 1:500 dilution) at 4°C overnight. The
556 sections were then washed three times with PBS and incubated with fluorescein-conjugated
557 secondary antibody (Thermo Fisher Scientific, Waltham, MA; Cat.: A10042; 1:500 dilution) for
558 1 hour at room temperature, then washed and mounted with DAPI-containing mounting media
559 (Vectashield, Vector Laboratories, Newark, CA; Cat.: H-1200-10). The slides were imaged on a
560 Zeiss LSM 900 confocal microscope (Carl Zeiss Microscopy, White Plains, NY). For the
561 quantification of the LAMP1 staining, the percentage of LAMP1-positive myofibers was
562 calculated and compared across treatment groups.

563 Nissl (toluidine blue) staining was used to study the morphology and pathology of neural tissue.
564 The spinal cord was harvested from mice, fixed in 4% paraformaldehyde (PFA) for 24 hours, and
565 then incubated in a solution containing 30% sucrose in PBS overnight, embedded in optimal
566 cutting temperature compound (OCT compound), and cryo-sectioned. Subsequently, the 10-
567 micron cryosections were stained with 1% toluidine blue containing 1% borate solution as
568 previously described[52,53]. Briefly, the slices were placed in Toluidine blue solution for 30 seconds
569 and rinsed in triple distilled water. Stained slices were examined using light microscopy.
570

571 **Statistical analysis**

572 Statistical analysis was performed using GraphPad Prism software (GraphPad Software, Boston,
573 MA), or RStudio software (RStudio, Boston, MA) in the case of Figure 1B. Unpaired t-test, one-
574 way ANOVA, or two-way ANOVA were used, as specified in the respective figure legends. p-

575 values lower than 0.05 were considered statistically significant; *: $p<0.05$, **: $p<0.01$, ***: $p < 0.005$, and ****: $p<0.0001$, ns= not significant. Error bars indicate the standard error of the mean (SEM).

578

579

580 **Legends**

581 **Figure 1. Gaa$^{-/-}$ mice show progressive accumulation of glycogen in skeletal muscle followed**
582 **by deterioration of muscle function.**

583 **A.** Glycogen content in quadriceps from Gaa$^{-/-}$ mice at 1, 2, and 3 months (mo) of age compared
584 to 1-month-old wild type (WT) C57BL/6 mice. n=5 per group, as indicated in parenthesis on the
585 x-axis. Statistical analysis was performed using unpaired t-test in GraphPad Prism software. **B.**
586 Graph illustrates the time that the mice spent on an accelerating rotarod before falling, to assess
587 muscle strength as the animals age from 2 to 14 months. The mean decline in motor function is
588 represented by the blue line within the shaded grey area, which indicates the SEM range. The
589 number of mice in each measurement group is indicated at the bottom of the graph (n). Statistical
590 analysis was performed using one-way ANOVA in GraphPad Prism software. *: $p<0.05$, **: $p <$
591 0.01, ***: $p < 0.005$, ****: $p < 0.001$.

592

593 **Figure 2. Early treatment of Gaa$^{-/-}$ mice with Gys1 ASOs lowers target mRNA and protein**
594 **expression, leading to reduced glycogen accumulation in skeletal muscle.**

595 **A.** Schematic illustration of the early treatment paradigm with Gys1 ASOs in Gaa$^{-/-}$ mice from 1
596 to 4.5 months of age. WT: wild type. **B.** qPCR analysis of Gys1 mRNA in quadriceps muscle. **C.**
597 Representative images of Western blot analysis of GYS1 protein in quadriceps, diaphragm, and
598 heart. The number of samples in each group is listed in parentheses on the x-axis. **D.** Glycogen
599 content measured using a biochemical assay in quadriceps muscle from Gaa$^{-/-}$ mice dosed with
600 either PBS, control ASO (Ctrl ASO), or two different Gys1 ASOs. The number of samples in each
601 group is listed in parentheses on the x-axis. **E.** Periodic acid-Schiff (PAS) staining of histological
602 sections of quadriceps muscle. Scale bars: 50 μm.

603 Statistical analysis was performed using unpaired t-test in GraphPad Prism software. ***: $p <$
604 0.005, ****: $p < 0.0001$.
605
606 **Figure 3. Therapeutic treatment with Gys1 ASO in Gaa$^{-/-}$ mice partially reverses glycogen**
607 **accumulation in skeletal muscle and preserves muscle strength.**
608 **A.** Schematic illustration of the reversal treatment paradigm with Gys1 ASO#2 in Gaa$^{-/-}$ mice from
609 3 to 6.5 months of age. WT: wild type. **B.** Graph illustrates the time that mice spent on an
610 accelerating rotarod before falling, to assess muscle strength. **C.** qPCR analysis of Gys1 mRNA.
611 The number of samples in each group is listed in parentheses on the x-axis. **D.** Representative
612 images of Western blot analysis of GYS1 protein in quadriceps, diaphragm, and heart. GAPDH
613 was used as loading control. **E.** Glycogen content measured using a biochemical assay in
614 quadriceps muscle from Gaa$^{-/-}$ mice dosed with either PBS, a control ASO (Ctrl ASO), or Gys1
615 ASO. The number of samples in each group is listed in parentheses on the x-axis. **F.** Representative
616 images from PAS staining of histological sections of quadriceps muscle. Scale bars: 50 µm.
617 Statistical analysis was performed using unpaired t-test in GraphPad Prism software. *: $p<0.05$,
618 ***: $p < 0.005$, ****: $p < 0.001$, ns: not significant.
619
620 **Figure 4. Combination treatment with Gys1 ASO and ERT reduces glycogen accumulation**
621 **and improves motor function in Gaa$^{-/-}$ mice.**
622 **A.** Schematic illustration of the study where 4-month-old Gaa$^{-/-}$ mice were dosed with Gys1
623 ASO#2 and ERT in combination. WT: wild type. **B**. Graph shows the results of a rotarod test to
624 assess muscle strength. The time that the mice spent on a rotating rod was recorded monthly over
625 the three months of treatment and expressed as percent change versus baseline measurements
626 (collected before the start of dosing) for each group; n=5 per group. Statistical analysis in B was

627 performed by two-way ANOVA using multiple comparisons in GraphPad Prism software. ****:
628 $p < 0.001$ between the $Gaa^{-/-}$ mice that received PBS and Gys1 ASO#2+ERT. **C.** Representative
629 images of Western blot analysis of GYS1 protein in quadriceps muscle, diaphragm, and heart.
630 GAPDH was used as loading control. **D.** Glycogen content measured using a biochemical assay in
631 quadriceps muscle and heart from wild type or $Gaa^{-/-}$ mice dosed with either PBS, Gys1 ASO#2,
632 Gys1 ASO#2+ERT, or ERT alone (n=5 per group).
633 Statistical analysis in C and D was performed using unpaired t-test. *: $p<0.05$, **: $p < 0.01$, ***:
634 $p < 0.005$, ns: not significant.
635
636 **Figure 5. Normalization of autophagic flux in skeletal muscle of Pompe mice after treatment**
637 **with Gys1 ASO, alone or in combination with ERT.**
638 **A**. Western blot analysis of LC3-II/LC3-I, p62, and LAMP1 proteins in quadriceps muscle and
639 heart from mice in cohort 3. GAPDH was used as loading control. The graphs illustrate the
640 quantification of Western blots from three independent experiments. WT: wild type. **B.**
641 Representative images of LAMP1 immunostaining in histological sections of quadriceps muscle
642 from $Gaa^{-/-}$ mice treated with Gys1 ASO#2, alone or in combination with ERT. The graph shows
643 the quantification of the stain as percentage of LAMP1-positive cells. LAMP1: lysosomal-
644 associated membrane protein 1. Statistical analysis was performed using unpaired t-test. *: $p<0.05$,
645 **: $p < 0.01$, ***: $p < 0.005$, ns: not significant.

646 **Figure 6**: **Model of pharmacological intervention in Pompe disease combining GYS1 ASO-**
647 **based SRT and ERT.**
648 We propose an adjunct therapeutic approach for Pompe disease based on the reduction of the
649 synthesis of new glycogen via GYS1 ASO-mediated SRT, combined with the ERT-mediated
650 clearance of pre-existing glycogen that has accumulated in the lysosome because of GAA
651 inactivation. Such combinatorial strategy would result in greater clinical benefit for Pompe
652 patients, especially in skeletal muscle, where ERT alone is not remarkably effective. SRT:
653 substrate reduction therapy; ERT: enzyme replacement therapy; GYS1: glycogen synthase 1;
654 ASO: antisense oligonucleotide; GAA: glucosidase, alpha acid; rhGAA: recombinant human
655 GAA.
656

657 **Supplementary Figure 1: Gys1 ASO#1 and ASO#2 knock down mouse Gys1 mRNA and**
658 **protein in wild type mice.**

659 **A.** Knockdown of mouse Gys1 mRNA measured by qPCR in quadriceps muscle of wild type mice
660 treated with ASO#1 and ASO#2 by subcutaneous injection at the indicated total weekly doses;
661 n=4 per group. **B.** Western blot analysis of GYS1 protein in gastrocnemius muscle of wild type
662 mice treated via subcutaneous injection with ASO#2 for 6 weeks at the indicated total weekly
663 doses; n=4 per group. The graph shows the quantification of GYS1 protein expression relative to
664 GAPDH (loading control) from three independent experiments. The GYS1 expression level after
665 treatment with control ASO (Ctrl ASO) at 100 mg/kg total weekly dose was used as reference and
666 was therefore set to 1. **C.** Western blot analysis of GYS1 protein in quadriceps muscle of $Gaa^{-/-}$
667 mice treated via subcutaneous injection with ASO#2 for 6 weeks at the indicated weekly doses;
668 n=3 per group. The PBS control group was used as reference to determine normal GYS1 levels
669 and was therefore set to 1. Representative blots from 3 sets of experiments are shown.

670 **Supplementary Figure 2. Schematic design of the treatment strategy and toxicity studies**
671 **using Gys1 ASO alone or in combination with ERT in Gaa-/- mice. Gys1 ASO and ERT are**
672 **well tolerated in Gaa$^{-/-}$ mice.**

673 **A.** Schematic illustration of the study used to assess the safety of the Gys1 ASOs in vivo. **B.**
674 Change in body weight of wild type and Gaa$^{-/-}$ mice dosed with either PBS, Gys1 ASO#2 alone,
675 or Gys1 ASO#2 in combination with ERT. The mice were dosed from 4 to 8 months of age, and
676 their body weights were recorded once every four weeks during the four-month study. **C.** Terminal
677 organ weight to body weight ratio normalized to wild type control group (set to 1). All the
678 treatments were well tolerated since the ratios are within two-fold of wild type. **D.** Serum
679 toxicology analysis performed at the end of the study shows no statistically significant change in
680 the treatment groups compared to control Gaa$^{-/-}$ mice dosed with PBS. The number of samples in
681 each group is listed in parentheses on the x-axis. ALT: alanine transaminase (values above 100
682 U/L are considered a sign of liver toxicity); AST: aspartate transaminase (values above 250-300
683 U/L are considered a sign of liver toxicity); BUN: blood urea nitrogen (values above 30 mmol/L
684 are considered a sign of kidney toxicity); CK: creatine kinase (values above 1,500 U/L are
685 considered a sign of muscle toxicity).

686

687

688 **Supplementary Figure 3. Histological analysis of spinal cord in 8-month-old Gaa$^{-/-}$ mice with**
689 **systemically delivered Gys1 ASO. No effect of systemically delivered Gys1 ASO in CNS.**
690 Nissl (toluidine blue) staining of histological sections of spinal cord from 8-months-old Gaa$^{-/-}$ mice
691 dosed by subcutaneous injection with 25 mg/kg of either control ASO or Gys1 ASO#2 once a
692 week for 16 weeks (16 total doses, 3.5 months of treatment, Cohort 2). Solid arrows indicate
693 swollen cell bodies in the cervical ventral horn; dashed arrows indicate activated glial cells;
694 asterisks indicate eccentric nuclei.
695
696

Supplementary Table 1. Summary of percent reduction over control ASO or PBS of Gys1 mRNA, glycogen content, and GYS1 protein in Gaa$^{-/-}$ mice treated with ASO, ASO+ERT, or ERT alone.

Mice from three separate cohorts were dosed with the indicated treatment, starting at 1, 3, or 4 months of age, and ending at 4.5, 6.5, or 8 months of age, respectively. The data is reported as percent reduction over control ASO or PBS of Gys1 mRNA, glycogen content, and GYS1 protein in Gaa$^{-/-}$ mice treated with ASO, ASO+ERT, or ERT alone

		% reduction					
		Gys1 mRNA (±95% C.I.)	**GYS1 protein**			**Glycogen content** (±95% C.I.)	
Mouse cohort	**Treatment**	**Quadriceps**	**Quadriceps**	**Diaphragm**	**Heart**	**Quadriceps**	**Heart**
1-month-old Gaa$^{-/-}$ (vs. Control ASO)	ASO#1 (n=12)	83.64 (77.40 - 88.16)	98	85	90	38.06 (14.50-61.07)	N.M.
	ASO#2 (n=12)	88.58 (83.61 - 92.06)	100	98	100	57.05 (35.57-71.36)	N.M.
3-month-old Gaa$^{-/-}$ (vs. Control ASO)	ASO#2 (n=10)	64.71 (57.00 - 71.05)	100	80	70	7.97 (5.53-28.45)	N.M.
4-month-old Gaa$^{-/-}$ (vs. PBS)	ASO#2 (n=5)	N.M.	100	90	100	55.22 (20.29-74.84)	14.03 (28.58-47.22)
	ASO#2+ERT (n=5)	N.M.	100	85	90	83.48 (53.80-94.10)	65.82 (5.88-87.59)
	ERT (n=5)	N.M.	0	0	0	15.78 (11.61-31.49)	74.93 (18.77-92.26)

697 N.M.: not measured; C.I: confidence interval.

698 **Supplementary Table 2. Summary of histological analyses.**

699 Semi-quantitative analysis of PAS staining, and percentage count of myofibers with a centralized

700 nucleus.

Mouse cohort	Genotype	Treatment	Quadriceps PAS score (1 to 4)	% Myofibers with centralized nucleus
1-month-old	$Gaa^{+/+}$	WT (n=5)	1	0
	$Gaa^{-/-}$	PBS (n=5)	2.2	8.4
		Ctrl ASO (n=5)	1.8	5.4
		ASO#1 (n=5)	1.4	14.1
		ASO#2 (n=5)	1	6.1
3-month-old	$Gaa^{+/+}$	WT (n=5)	1	0.7
	$Gaa^{-/-}$	PBS (n=5)	3.2	25.7
		Ctrl ASO (n=5)	2.2	19.6
		ASO#2 (n=5)	1.25	23.4
4-month-old	$Gaa^{+/+}$	WT (n=4)	1	1.4
	$Gaa^{-/-}$	PBS (n=4)	3.75	26.9
		ASO#2 (n=4)	1.5	25.2
		ASO#2+ERT (n=4)	1	16
		ERT (n=4)	3	17.9

References

1. Tang, H., Feuchtbaum, L., Sciortino, S., Matteson, J., Mathur, D., Bishop, T., and Olney, R.S. (2020). The First Year Experience of Newborn Screening for Pompe Disease in California. Int J Neonatal Screen *6*, 9. 10.3390/ijns6010009.
2. Raben, N., Nichols, R.C., Boerkoel, C., and Plotz, P. (1995). Genetic defects in patients with glycogenosis type II (acid maltase deficiency). Muscle Nerve Suppl *3*, S70-74.
3. Kroos, M.A., Van der Kraan, M., Van Diggelen, O.P., Kleijer, W.J., Reuser, A.J., Van den Boogaard, M.J., Ausems, M.G., Ploos van Amstel, H.K., Poenaru, L., Nicolino, M., and et al. (1995). Glycogen storage disease type II: frequency of three common mutant alleles and their associated clinical phenotypes studied in 121 patients. J Med Genet *32*, 836-837.
4. Raben, N., Nagaraju, K., Lee, E., Kessler, P., Byrne, B., Lee, L., LaMarca, M., King, C., Ward, J., Sauer, B., and Plotz, P. (1998). Targeted disruption of the acid alpha-glucosidase gene in mice causes an illness with critical features of both infantile and adult human glycogen storage disease type II. J Biol Chem *273*, 19086-19092.
5. Prater, S.N., Patel, T.T., Buckley, A.F., Mandel, H., Vlodavski, E., Banugaria, S.G., Feeney, E.J., Raben, N., and Kishnani, P.S. (2013). Skeletal muscle pathology of infantile Pompe disease during long-term enzyme replacement therapy. Orphanet J Rare Dis *8*, 90. 10.1186/1750-1172-8-90.
6. Bellotti, A.S., Andreoli, L., Ronchi, D., Bresolin, N., Comi, G.P., and Corti, S. (2020). Molecular Approaches for the Treatment of Pompe Disease. Mol Neurobiol *57*, 1259-1280. 10.1007/s12035-019-01820-5.
7. Xu, S., Lun, Y., Frascella, M., Garcia, A., Soska, R., Nair, A., Ponery, A.S., Schilling, A., Feng, J., Tuske, S., et al. (2019). Improved efficacy of a next-generation ERT in murine Pompe disease. JCI Insight *4*. 10.1172/jci.insight.125358.
8. Kuperus, E., Kruijshaar, M.E., Wens, S.C.A., de Vries, J.M., Favejee, M.M., van der Meijden, J.C., Rizopoulos, D., Brusse, E., van Doorn, P.A., van der Ploeg, A.T., and van der Beek, N. (2017). Long-term benefit of enzyme replacement therapy in Pompe disease: A 5-year prospective study. Neurology *89*, 2365-2373. 10.1212/WNL.0000000000004711.
9. Alandy-Dy, J., Wencel, M., Hall, K., Simon, J., Chen, Y., Valenti, E., Yang, J., Bali, D., Lakatos, A., Goyal, N., et al. (2019). Variable clinical features and genotype-phenotype correlations in 18 patients with late-onset Pompe disease. Ann Transl Med *7*, 276. 10.21037/atm.2019.06.48.
10. Raben, N., Fukuda, T., Gilbert, A.L., de Jong, D., Thurberg, B.L., Mattaliano, R.J., Meikle, P., Hopwood, J.J., Nagashima, K., Nagaraju, K., and Plotz, P.H. (2005). Replacing acid alpha-glucosidase in Pompe disease: recombinant and transgenic enzymes are equipotent, but neither completely clears glycogen from type II muscle fibers. Mol Ther *11*, 48-56. 10.1016/j.ymthe.2004.09.017.
11. Miller, C.M., and Harris, E.N. (2016). Antisense Oligonucleotides: Treatment Strategies and Cellular Internalization. RNA Dis *3*. 10.14800/rd.1393.
12. Drost, M.R., Schaart, G., van Dijk, P., van Capelle, C.I., van der Vusse, G.J., Delhaas, T., van der Ploeg, A.T., and Reuser, A.J. (2008). Both type 1 and type 2a muscle fibers can respond to enzyme therapy in Pompe disease. Muscle Nerve *37*, 251-255. 10.1002/mus.20896.
13. Taylor, K.M., Meyers, E., Phipps, M., Kishnani, P.S., Cheng, S.H., Scheule, R.K., and Moreland, R.J. (2013). Dysregulation of multiple facets of glycogen metabolism in a murine model of Pompe disease. PLoS One *8*, e56181. 10.1371/journal.pone.0056181.
14. Canibano-Fraile, R., Harlaar, L., Dos Santos, C.A., Hoogeveen-Westerveld, M., Demmers, J.A.A., Snijders, T., Lijnzaad, P., Verdijk, R.M., van der Beek, N., van Doorn, P.A., et al. (2023). Lysosomal

748 glycogen accumulation in Pompe disease results in disturbed cytoplasmic glycogen metabolism.
749 J Inherit Metab Dis *46*, 101-115. 10.1002/jimd.12560.
750 15. van der Ploeg, A., Carlier, P.G., Carlier, R.Y., Kissel, J.T., Schoser, B., Wenninger, S., Pestronk, A.,
751 Barohn, R.J., Dimachkie, M.M., Goker-Alpan, O., et al. (2016). Prospective exploratory muscle
752 biopsy, imaging, and functional assessment in patients with late-onset Pompe disease treated
753 with alglucosidase alfa: The EMBASSY Study. Mol Genet Metab *119*, 115-123.
754 10.1016/j.ymgme.2016.05.013.
755 16. Clayton, N.P., Nelson, C.A., Weeden, T., Taylor, K.M., Moreland, R.J., Scheule, R.K., Phillips, L.,
756 Leger, A.J., Cheng, S.H., and Wentworth, B.M. (2014). Antisense Oligonucleotide-mediated
757 Suppression of Muscle Glycogen Synthase 1 Synthesis as an Approach for Substrate Reduction
758 Therapy of Pompe Disease. Mol Ther Nucleic Acids *3*, e206. 10.1038/mtna.2014.57.
759 17. Douillard-Guilloux, G., Raben, N., Takikita, S., Ferry, A., Vignaud, A., Guillet-Deniau, I., Favier, M.,
760 Thurberg, B.L., Roach, P.J., Caillaud, C., and Richard, E. (2010). Restoration of muscle
761 functionality by genetic suppression of glycogen synthesis in a murine model of Pompe disease.
762 Hum Mol Genet *19*, 684-696. 10.1093/hmg/ddp535.
763 18. Meena, N.K., Randazzo, D., Raben, N., and Puertollano, R. (2023). AAV-mediated delivery of
764 secreted acid alpha-glucosidase with enhanced uptake corrects neuromuscular pathology in
765 Pompe mice. JCI Insight *8*. 10.1172/jci.insight.170199.
766 19. Douillard-Guilloux, G., Raben, N., Takikita, S., Batista, L., Caillaud, C., and Richard, E. (2008).
767 Modulation of glycogen synthesis by RNA interference: towards a new therapeutic approach for
768 glycogenosis type II. Hum Mol Genet *17*, 3876-3886. 10.1093/hmg/ddn290.
769 20. Crooke, S.T., Baker, B.F., Pham, N.C., Hughes, S.G., Kwoh, T.J., Cai, D., Tsimikas, S., Geary, R.S.,
770 and Bhanot, S. (2018). The Effects of 2'-O-Methoxyethyl Oligonucleotides on Renal Function in
771 Humans. Nucleic Acid Ther *28*, 10-22. 10.1089/nat.2017.0693.
772 21. Crooke, S.T., Baker, B.F., Xia, S., Yu, R.Z., Viney, N.J., Wang, Y., Tsimikas, S., and Geary, R.S.
773 (2019). Integrated Assessment of the Clinical Performance of GalNAc(3)-Conjugated 2'-O-
774 Methoxyethyl Chimeric Antisense Oligonucleotides: I. Human Volunteer Experience. Nucleic
775 Acid Ther *29*, 16-32. 10.1089/nat.2018.0753.
776 22. Crooke, S.T., Liang, X.H., Baker, B.F., and Crooke, R.M. (2021). Antisense technology: A review. J
777 Biol Chem *296*, 100416. 10.1016/j.jbc.2021.100416.
778 23. Shen, W., De Hoyos, C.L., Migawa, M.T., Vickers, T.A., Sun, H., Low, A., Bell, T.A., 3rd, Rahdar, M.,
779 Mukhopadhyay, S., Hart, C.E., et al. (2019). Chemical modification of PS-ASO therapeutics
780 reduces cellular protein-binding and improves the therapeutic index. Nat Biotechnol *37*, 640-
781 650. 10.1038/s41587-019-0106-2.
782 24. Crooke, S.T., Vickers, T.A., and Liang, X.H. (2020). Phosphorothioate modified oligonucleotide-
783 protein interactions. Nucleic Acids Res *48*, 5235-5253. 10.1093/nar/gkaa299.
784 25. Ramms, B., Patel, S., Sun, X., Pessentheiner, A.R., Ducasa, G.M., Mullick, A.E., Lee, R.G., Crooke,
785 R.M., Tsimikas, S., Witztum, J.L., and Gordts, P.L. (2022). Interventional hepatic apoC-III
786 knockdown improves atherosclerotic plaque stability and remodeling by triglyceride lowering.
787 JCI Insight *7*. 10.1172/jci.insight.158414.
788 26. Walsh, M., Bethune, C., Smyth, A., Tyrwhitt, J., Jung, S.W., Yu, R.Z., Wang, Y., Geary, R.S., Weitz,
789 J., Bhanot, S., and Investigators, C.S. (2022). Phase 2 Study of the Factor XI Antisense Inhibitor
790 IONIS-FXI(Rx) in Patients With ESRD. Kidney Int Rep *7*, 200-209. 10.1016/j.ekir.2021.11.011.
791 27. Nitschke, S., Sullivan, M.A., Mitra, S., Marchioni, C.R., Lee, J.P.Y., Smith, B.H., Ahonen, S., Wu, J.,
792 Chown, E.E., Wang, P., et al. (2022). Glycogen synthase downregulation rescues the
793 amylopectinosis of murine RBCK1 deficiency. Brain *145*, 2361-2377. 10.1093/brain/awac017.
794 28. Karam, C., Brown, D., Yang, M., Done, N., Zhu, J.J., Greatsinger, A., Bozas, A., Vera-Llonch, M.,
795 and Signorovitch, J. (2022). Long-term treatment effects of inotersen on health-related quality

796 of life in patients with hATTR amyloidosis with polyneuropathy: Analysis of the open-label
797 extension of the NEURO-TTR trial. Muscle Nerve *66*, 438-446. 10.1002/mus.27675.
798 29. Karam, C., Brown, D., Yang, M., Done, N., Dieye, I., Bozas, A., Vera Llonch, M., and Signorovitch,
799 J. (2022). Factors associated with increased health-related quality-of-life benefits in hereditary
800 transthyretin amyloidosis polyneuropathy patients treated with inotersen. Muscle Nerve *66*,
801 319-328. 10.1002/mus.27668.
802 30. Raben, N., Nagaraju, K., Lee, E., and Plotz, P. (2000). Modulation of disease severity in mice with
803 targeted disruption of the acid alpha-glucosidase gene. Neuromuscul Disord *10*, 283-291.
804 31. Raben, N., Ralston, E., Chien, Y.H., Baum, R., Schreiner, C., Hwu, W.L., Zaal, K.J., and Plotz, P.H.
805 (2010). Differences in the predominance of lysosomal and autophagic pathologies between
806 infants and adults with Pompe disease: implications for therapy. Mol Genet Metab *101*, 324-
807 331. 10.1016/j.ymgme.2010.08.001.
808 32. Lim, J.A., Sun, B., Puertollano, R., and Raben, N. (2018). Therapeutic Benefit of Autophagy
809 Modulation in Pompe Disease. Mol Ther *26*, 1783-1796. 10.1016/j.ymthe.2018.04.025.
810 33. Pugsley, H.R. (2017). Assessing Autophagic Flux by Measuring LC3, p62, and LAMP1 Co-
811 localization Using Multispectral Imaging Flow Cytometry. J Vis Exp. 10.3791/55637.
812 34. Pugsley, H.R. (2017). Quantifying autophagy: Measuring LC3 puncta and autolysosome
813 formation in cells using multispectral imaging flow cytometry. Methods *112*, 147-156.
814 10.1016/j.ymeth.2016.05.022.
815 35. Korlimarla, A., Lim, J.A., Kishnani, P.S., and Sun, B. (2019). An emerging phenotype of central
816 nervous system involvement in Pompe disease: from bench to bedside and beyond. Ann Transl
817 Med *7*, 289. 10.21037/atm.2019.04.49.
818 36. Chien, Y.H., Hwu, W.L., and Lee, N.C. (2013). Pompe disease: early diagnosis and early treatment
819 make a difference. Pediatr Neonatol *54*, 219-227. 10.1016/j.pedneo.2013.03.009.
820 37. Lim, K.R., Maruyama, R., and Yokota, T. (2017). Eteplirsen in the treatment of Duchenne
821 muscular dystrophy. Drug Des Devel Ther *11*, 533-545. 10.2147/DDDT.S97635.
822 38. Mendell, J.R., Rodino-Klapac, L.R., Sahenk, Z., Roush, K., Bird, L., Lowes, L.P., Alfano, L., Gomez,
823 A.M., Lewis, S., Kota, J., et al. (2013). Eteplirsen for the treatment of Duchenne muscular
824 dystrophy. Ann Neurol *74*, 637-647. 10.1002/ana.23982.
825 39. Sazani, P., Ness, K.P., Weller, D.L., Poage, D., Nelson, K., and Shrewsbury, A.S. (2011). Chemical
826 and mechanistic toxicology evaluation of exon skipping phosphorodiamidate morpholino
827 oligomers in mdx mice. Int J Toxicol *30*, 322-333. 10.1177/1091581811403504.
828 40. Frank, D.E., Schnell, F.J., Akana, C., El-Husayni, S.H., Desjardins, C.A., Morgan, J., Charleston, J.S.,
829 Sardone, V., Domingos, J., Dickson, G., et al. (2020). Increased dystrophin production with
830 golodirsen in patients with Duchenne muscular dystrophy. Neurology *94*, e2270-e2282.
831 10.1212/WNL.0000000000009233.
832 41. Clemens, P.R., Rao, V.K., Connolly, A.M., Harper, A.D., Mah, J.K., Smith, E.C., McDonald, C.M.,
833 Zaidman, C.M., Morgenroth, L.P., Osaki, H., et al. (2020). Safety, Tolerability, and Efficacy of
834 Viltolarsen in Boys With Duchenne Muscular Dystrophy Amenable to Exon 53 Skipping: A Phase
835 2 Randomized Clinical Trial. JAMA Neurol *77*, 982-991. 10.1001/jamaneurol.2020.1264.
836 42. Finkel, R.S., Mercuri, E., Darras, B.T., Connolly, A.M., Kuntz, N.L., Kirschner, J., Chiriboga, C.A.,
837 Saito, K., Servais, L., Tizzano, E., et al. (2017). Nusinersen versus Sham Control in Infantile-Onset
838 Spinal Muscular Atrophy. N Engl J Med *377*, 1723-1732. 10.1056/NEJMoa1702752.
839 43. Hua, Y., Sahashi, K., Hung, G., Rigo, F., Passini, M.A., Bennett, C.F., and Krainer, A.R. (2010).
840 Antisense correction of SMN2 splicing in the CNS rescues necrosis in a type III SMA mouse
841 model. Genes Dev *24*, 1634-1644. 10.1101/gad.1941310.
842 44. van der Wal, E., Bergsma, A.J., Pijnenburg, J.M., van der Ploeg, A.T., and Pijnappel, W. (2017).
843 Antisense Oligonucleotides Promote Exon Inclusion and Correct the Common c.-32-13T>G GAA

844 Splicing Variant in Pompe Disease. Mol Ther Nucleic Acids *7*, 90-100.
845 10.1016/j.omtn.2017.03.001.
846 45. van der Wal, E., Bergsma, A.J., van Gestel, T.J.M., In 't Groen, S.L.M., Zaehres, H., Arauzo-Bravo,
847 M.J., Scholer, H.R., van der Ploeg, A.T., and Pijnappel, W. (2017). GAA Deficiency in Pompe
848 Disease Is Alleviated by Exon Inclusion in iPSC-Derived Skeletal Muscle Cells. Mol Ther Nucleic
849 Acids *7*, 101-115. 10.1016/j.omtn.2017.03.002.
850 46. Goina, E., Peruzzo, P., Bembi, B., Dardis, A., and Buratti, E. (2017). Glycogen Reduction in
851 Myotubes of Late-Onset Pompe Disease Patients Using Antisense Technology. Mol Ther *25*,
852 2117-2128. 10.1016/j.ymthe.2017.05.019.
853 47. Moulton, H.M., and Moulton, J.D. (2010). Morpholinos and their peptide conjugates:.
854 Biochimica et Biophysica Acta, 2296-2303.
855 48. Ullman, J.C., Mellem, K.T., Xi, Y., Ramanan, V., Merritt, H., Choy, R., Gujral, T., Young, L.E.A.,
856 Blake, K., Tep, S., et al. (2024). Small-molecule inhibition of glycogen synthase 1 for the
857 treatment of Pompe disease and other glycogen storage disorders. Sci Transl Med *16*, eadf1691.
858 10.1126/scitranslmed.adf1691.
859 49. Baker, B.F., Lot, S.S., Condon, T.P., Cheng-Flournoy, S., Lesnik, E.A., Sasmor, H.M., and Bennett,
860 C.F. (1997). 2'-O-(2-Methoxy)ethyl-modified anti-intercellular adhesion molecule 1 (ICAM-1)
861 oligonucleotides selectively increase the ICAM-1 mRNA level and inhibit formation of the ICAM-
862 1 translation initiation complex in human umbilical vein endothelial cells. J Biol Chem *272*,
863 11994-12000. 10.1074/jbc.272.18.11994.
864 50. Raben, N., Lu, N., Nagaraju, K., Rivera, Y., Lee, A., Yan, B., Byrne, B., Meikle, P.J.,
865 Umapathysivam, K., Hopwood, J.J., and Plotz, P.H. (2001). Conditional tissue-specific expression
866 of the acid alpha-glucosidase (GAA) gene in the GAA knockout mice: implications for therapy.
867 Hum Mol Genet *10*, 2039-2047.
868 51. Tresse, E., Salomons, F.A., Vesa, J., Bott, L.C., Kimonis, V., Yao, T.P., Dantuma, N.P., and Taylor,
869 J.P. (2010). VCP/p97 is essential for maturation of ubiquitin-containing autophagosomes and
870 this function is impaired by mutations that cause IBMPFD. Autophagy *6*, 217-227.
871 52. Cheng, C., Weiss, L., Leinonen, H., Shmara, A., Yin, H.Z., Ton, T., Do, A., Lee, J., Ta, L., Mohanty,
872 E., et al. (2022). VCP/p97 inhibitor CB-5083 modulates muscle pathology in a mouse model of
873 VCP inclusion body myopathy. J Transl Med *20*, 21. 10.1186/s12967-021-03186-6.
874 53. Yin, H.Z., Wang, H.L., Ji, S.G., Medvedeva, Y.V., Tian, G., Bazrafkan, A.K., Maki, N.Z., Akbari, Y.,
875 and Weiss, J.H. (2019). Rapid Intramitochondrial Zn2+ Accumulation in CA1 Hippocampal
876 Pyramidal Neurons After Transient Global Ischemia: A Possible Contributor to Mitochondrial
877 Disruption and Cell Death. J Neuropathol Exp Neurol *78*, 655-664. 10.1093/jnen/nlz042.

878

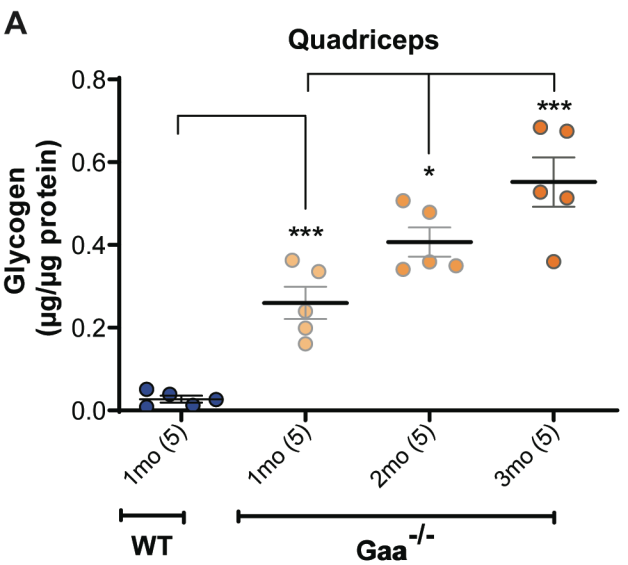
A
Quadriceps
Glycogen (µg/µg protein)
0.8
0.6
0.4
0.2
0.0
***
*
***
1mo (5)
1mo (5)
2mo (5)
3mo (5)
WT
Gaa-/-

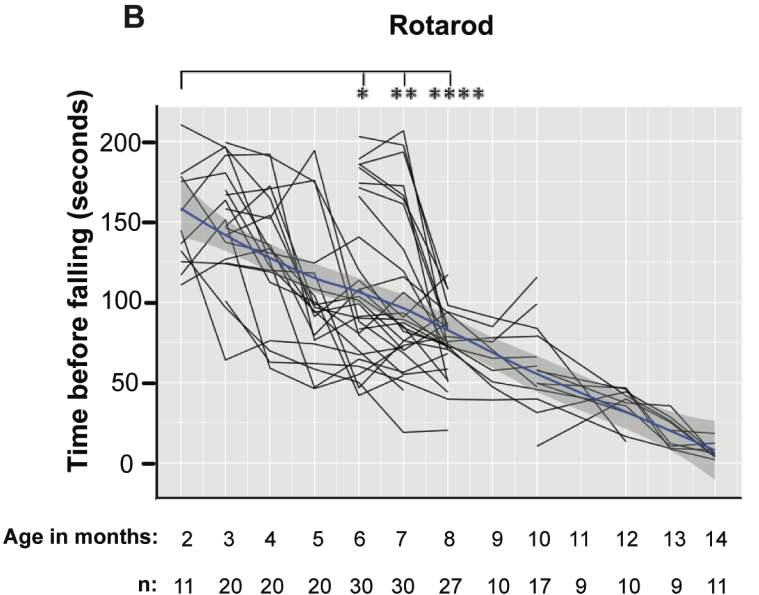
B
Rotarod
Time before falling (seconds)
200
150
100
50
0
* ** ****
Age in months: 2 3 4 5 6 7 8 9 10 11 12 13 14
n: 11 20 20 20 30 30 27 10 17 9 10 9 11

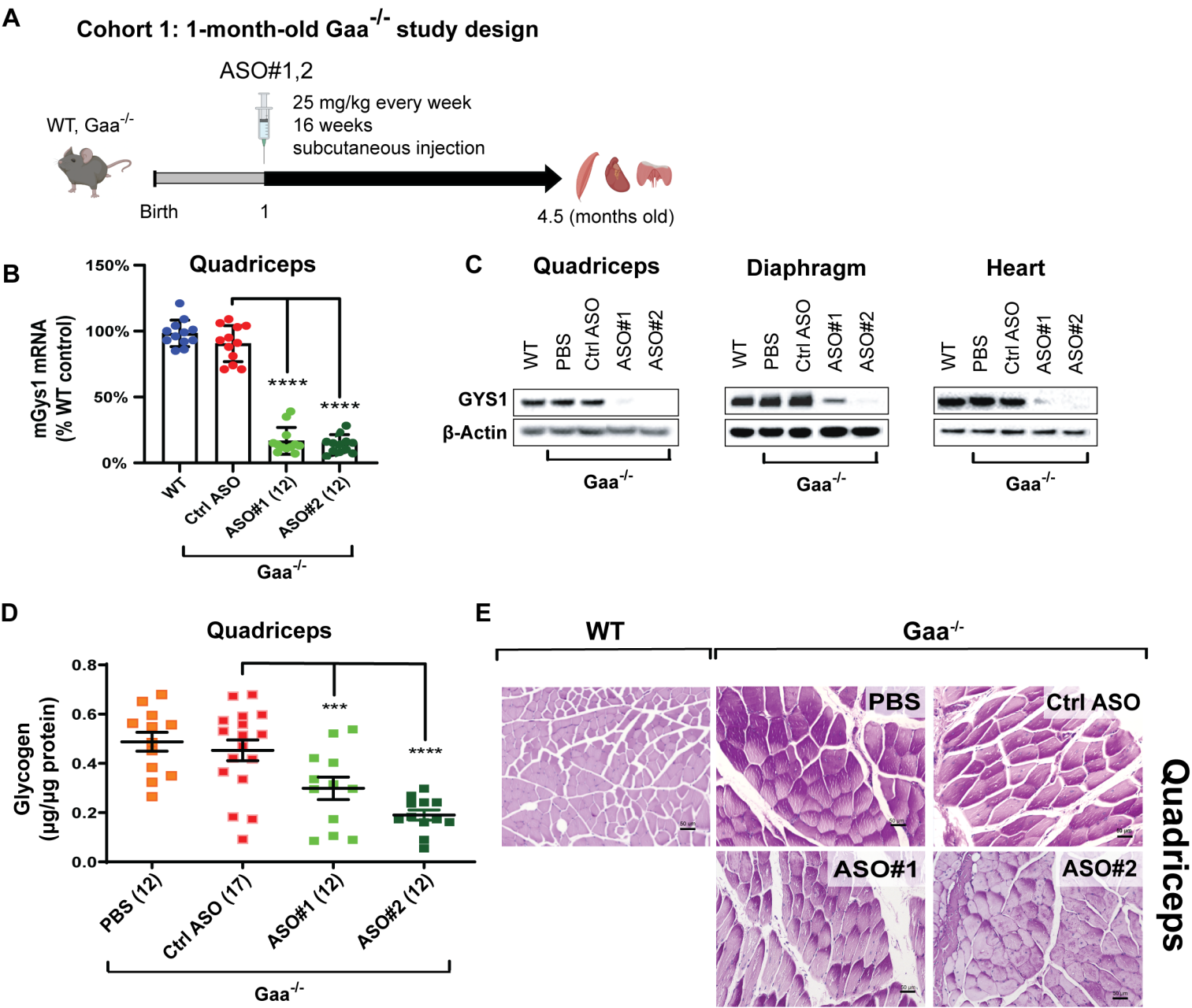
A
Cohort 1: 1-month-old Gaa-/- study design
ASO#1,2
25 mg/kg every week
16 weeks
subcutaneous injection
WT, Gaa-/-
Birth
1
4.5 (months old)
B
Quadriceps
mGys1 mRNA (% WT control)
150%
100%
50%
0%
****
****
WT
Ctrl ASO
ASO#1 (12)
ASO#2 (12)
Gaa-/-
C
Quadriceps
Diaphragm
Heart
WT
PBS
Ctrl ASO
ASO#1
ASO#2
GYS1
β-Actin
Gaa-/-
D
Quadriceps
Glycogen (µg/µg protein)
0.8
0.6
0.4
0.2
0.0
***
****
PBS (12)
Ctrl ASO (17)
ASO#1 (12)
ASO#2 (12)
Gaa-/-
E
WT
Gaa-/-
PBS
Ctrl ASO
ASO#1
ASO#2
Quadriceps

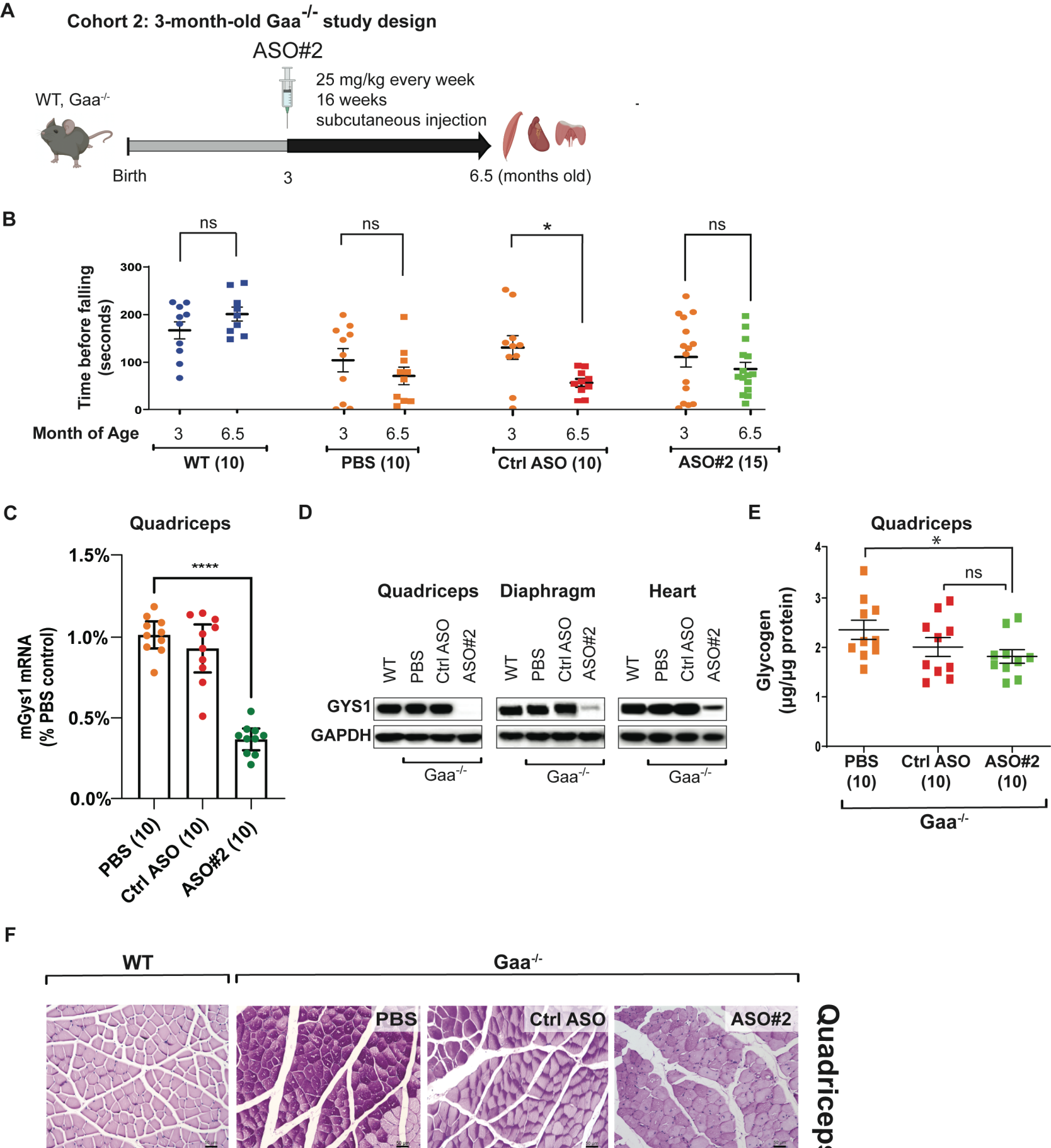
A
Cohort 2: 3-month-old Gaa-/- study design
ASO#2
25 mg/kg every week
16 weeks
subcutaneous injection
WT, Gaa-/-
Birth
3
6.5 (months old)
B
ns
ns
*
ns
Time before falling (seconds)
300
200
100
0
Month of Age
3
6.5
WT (10)
PBS (10)
Ctrl ASO (10)
ASO#2 (15)
C
Quadriceps
****
mGys1 mRNA (% PBS control)
1.5%
1.0%
0.5%
0.0%
PBS (10)
Ctrl ASO (10)
ASO#2 (10)
D
Quadriceps
Diaphragm
Heart
WT
PBS
Ctrl ASO
ASO#2
GYS1
GAPDH
Gaa-/-
E
Quadriceps
*
ns
Glycogen (µg/µg protein)
4
3
2
1
0
PBS (10)
Ctrl ASO (10)
ASO#2 (10)
Gaa-/-
F
WT
Gaa-/-
PBS
Ctrl ASO
ASO#2
Quadriceps

A

Cohort 3: 5-month-old Gaa$^{-/-}$ adjunct treatment study design

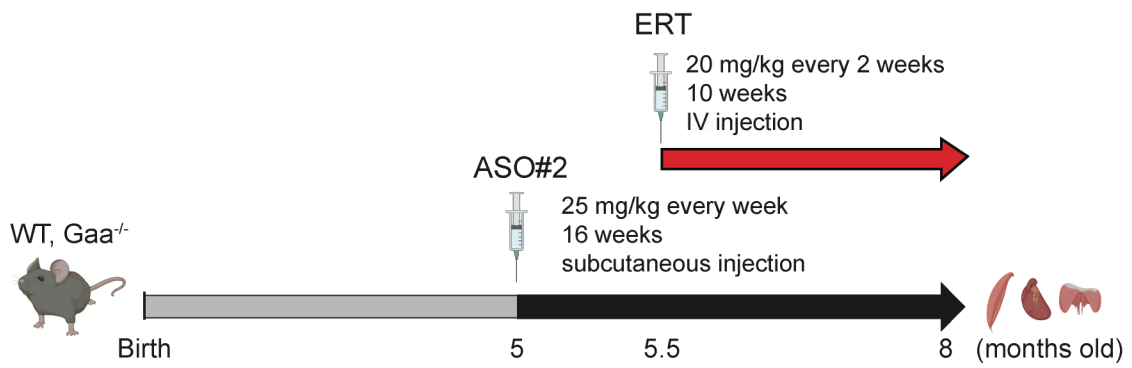

B

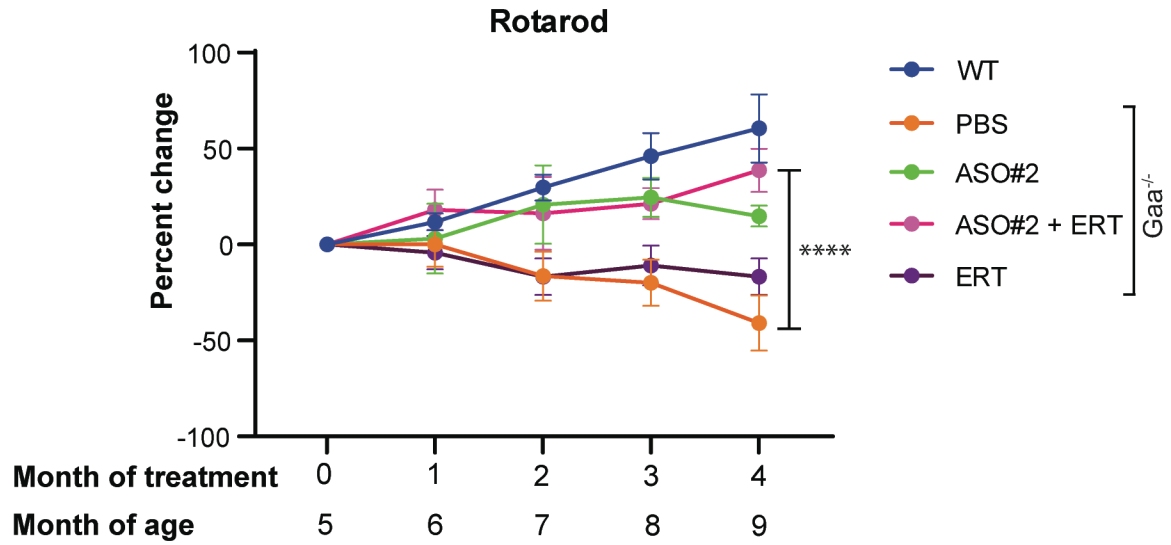

C

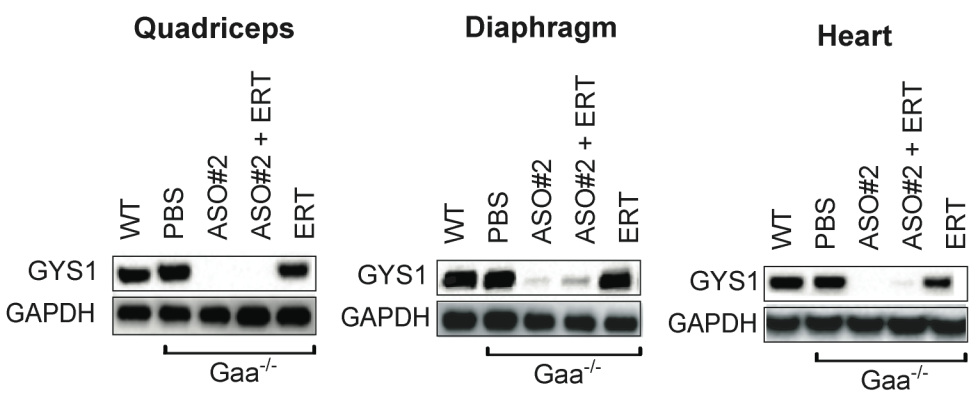

D

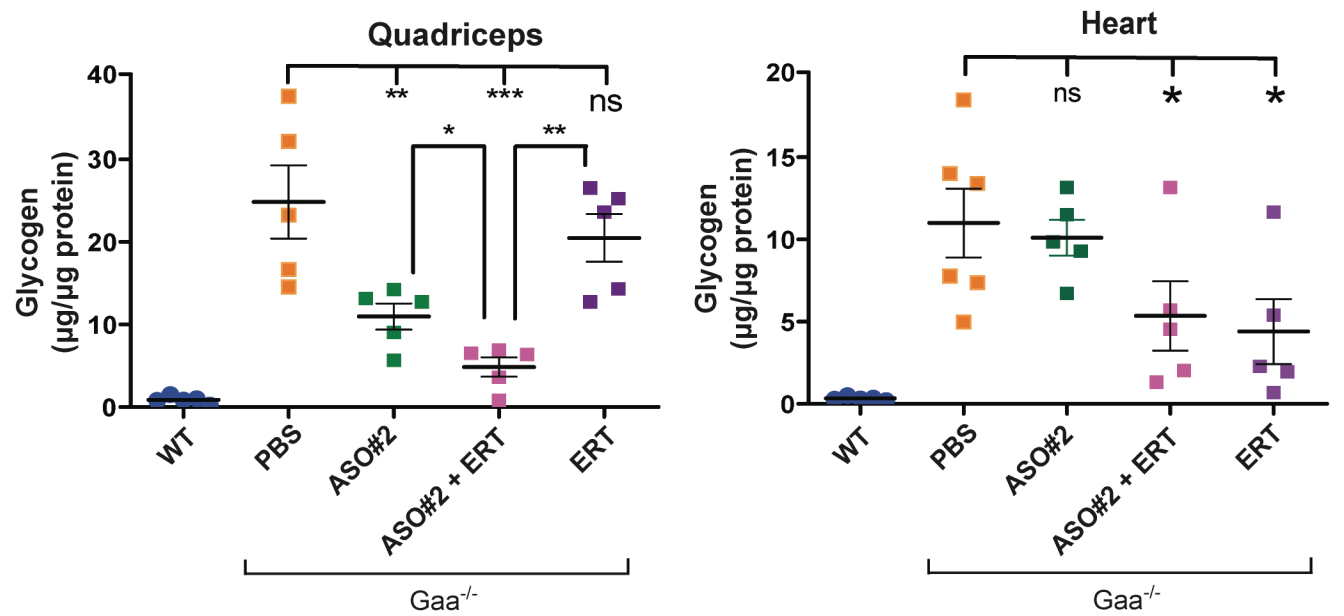

E

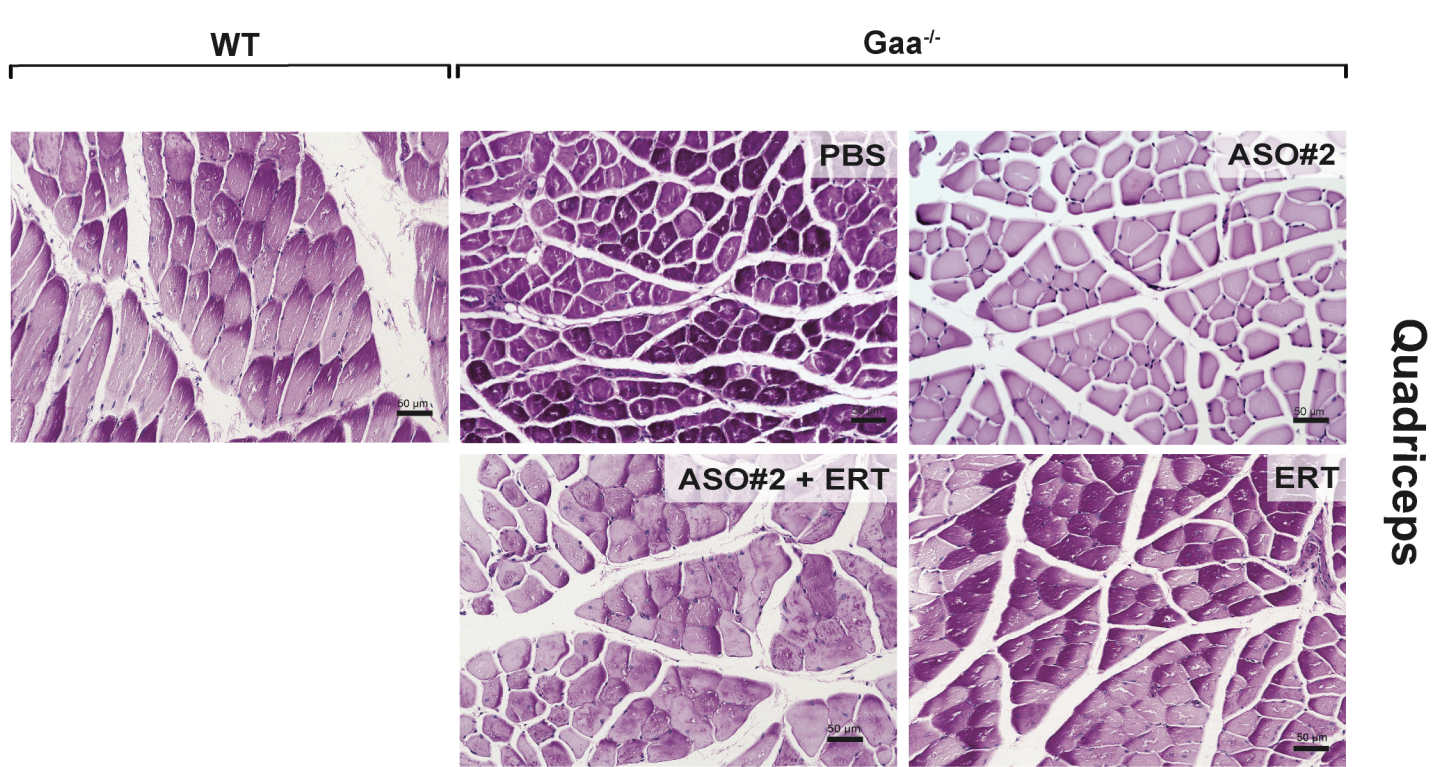

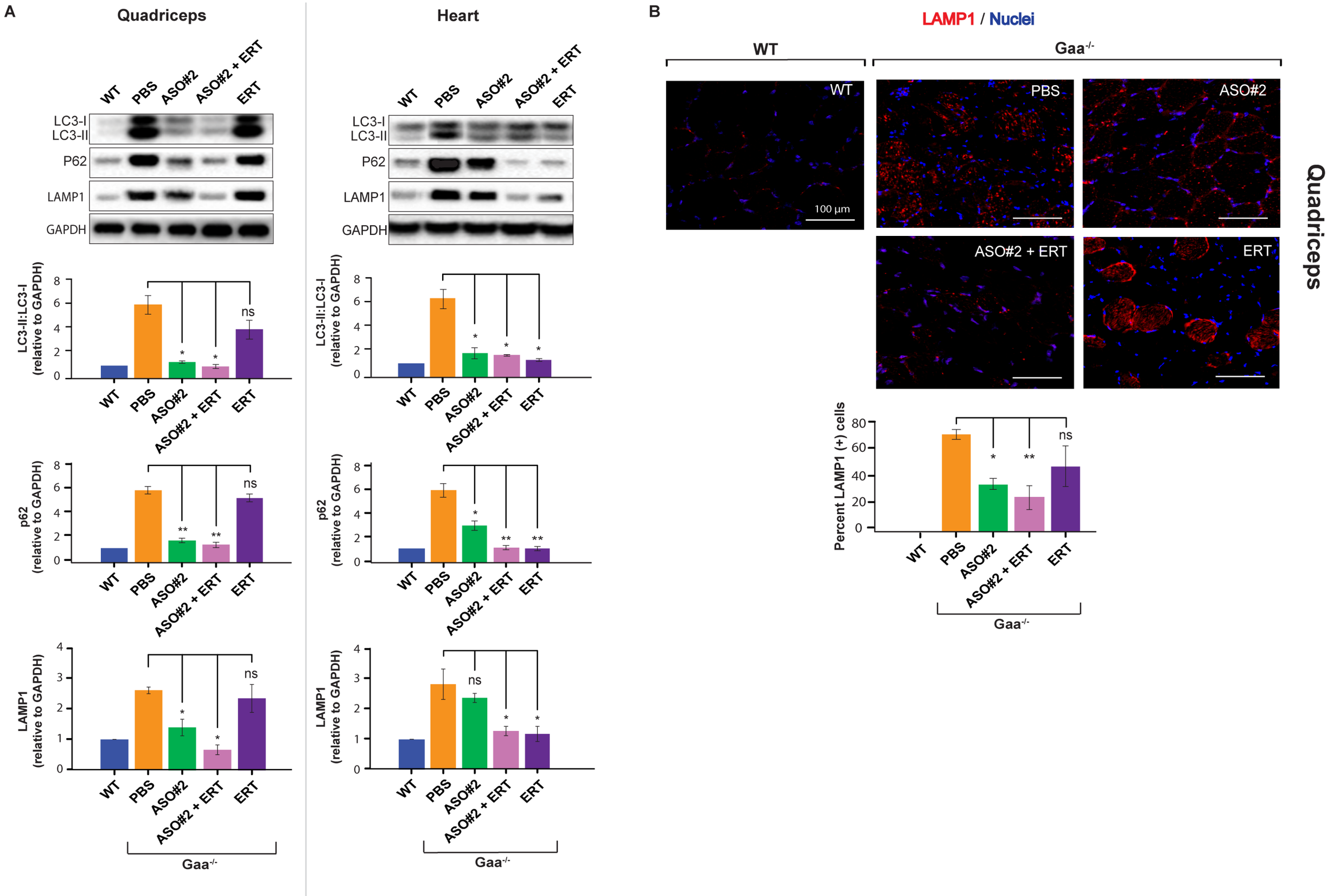
A
Quadriceps
Heart
WT
PBS
ASO#2
ASO#2 + ERT
ERT
LC3-I
LC3-II
P62
LAMP1
GAPDH
LC3-II:LC3-I (relative to GAPDH)
p62 (relative to GAPDH)
LAMP1 (relative to GAPDH)
ns
Gaa-/-
B
LAMP1 / Nuclei
WT
Gaa-/-
100 µm
Percent LAMP1 (+) cells
Quadriceps

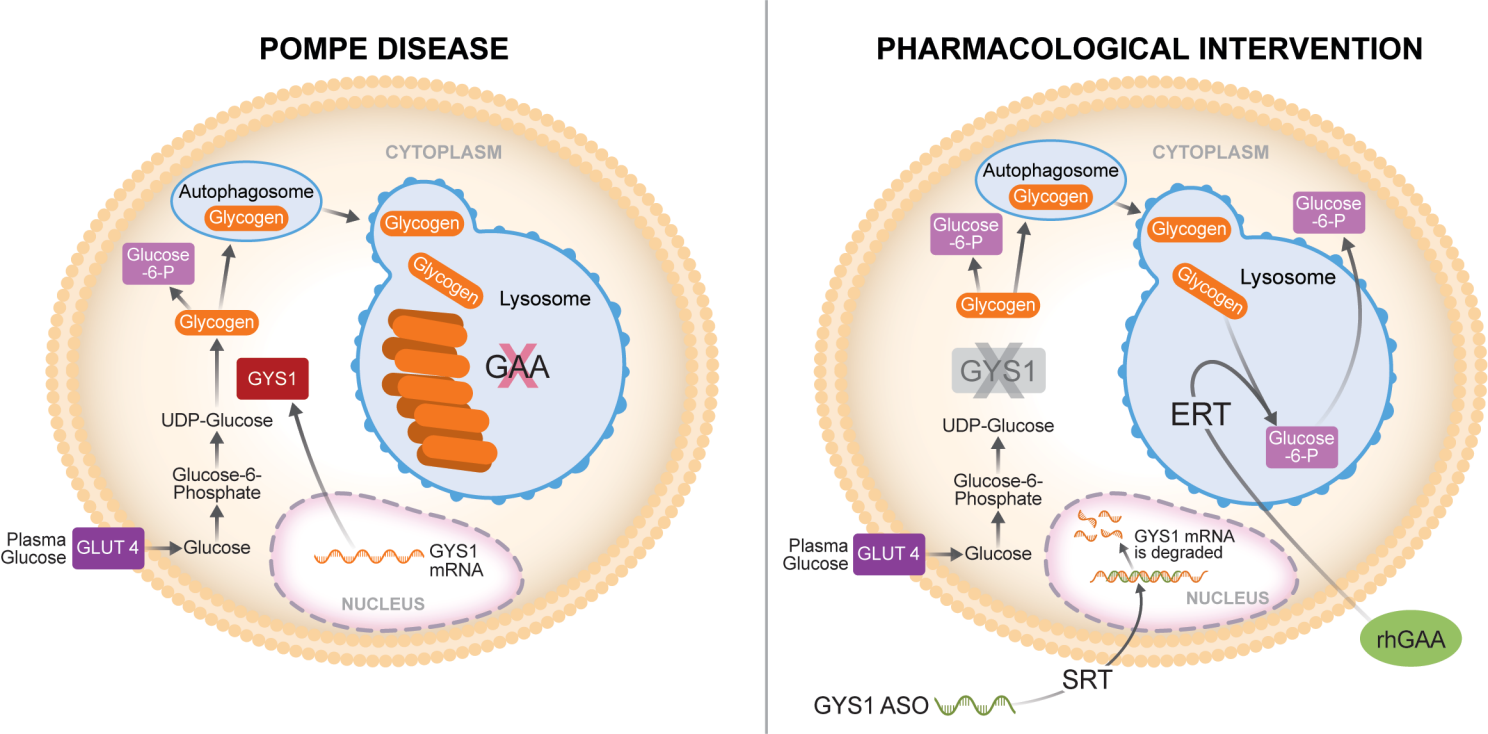
POMPE DISEASE
CYTOPLASM
Autophagosome
Glycogen
Glucose -6-P
Glycogen
Glycogen
Glycogen
Lysosome
GAA
GYS1
UDP-Glucose
Glucose-6-Phosphate
Plasma Glucose
GLUT 4
Glucose
GYS1 mRNA
NUCLEUS
PHARMACOLOGICAL INTERVENTION
CYTOPLASM
Autophagosome
Glycogen
Glucose -6-P
Glycogen
Glucose -6-P
Glycogen
Glycogen
Lysosome
GYS1
ERT
Glucose -6-P
UDP-Glucose
Glucose-6-Phosphate
Plasma Glucose
GLUT 4
Glucose
GYS1 mRNA is degraded
NUCLEUS
rhGAA
SRT
GYS1 ASO

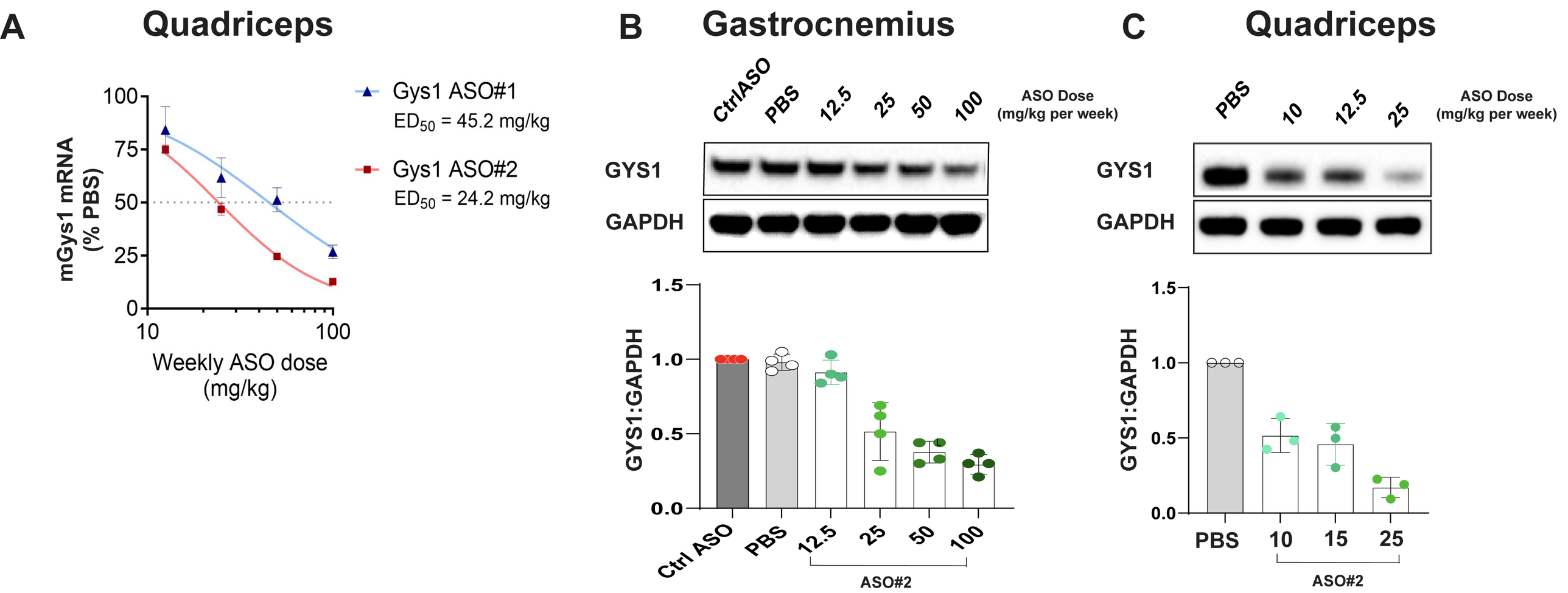
A
Quadriceps
mGys1 mRNA (% PBS)
100
75
50
25
0
10
100
Weekly ASO dose (mg/kg)
Gys1 ASO#1
ED50 = 45.2 mg/kg
Gys1 ASO#2
ED50 = 24.2 mg/kg
B
Gastrocnemius
CtrlASO
PBS
12.5
25
50
100
ASO Dose (mg/kg per week)
GYS1
GAPDH
GYS1:GAPDH
1.5
1.0
0.5
0.0
Ctrl ASO
PBS
12.5
25
50
100
ASO#2
C
Quadriceps
PBS
10
12.5
25
ASO Dose (mg/kg per week)
GYS1
GAPDH
GYS1:GAPDH
1.5
1.0
0.5
0.0
PBS
10
15
25
ASO#2

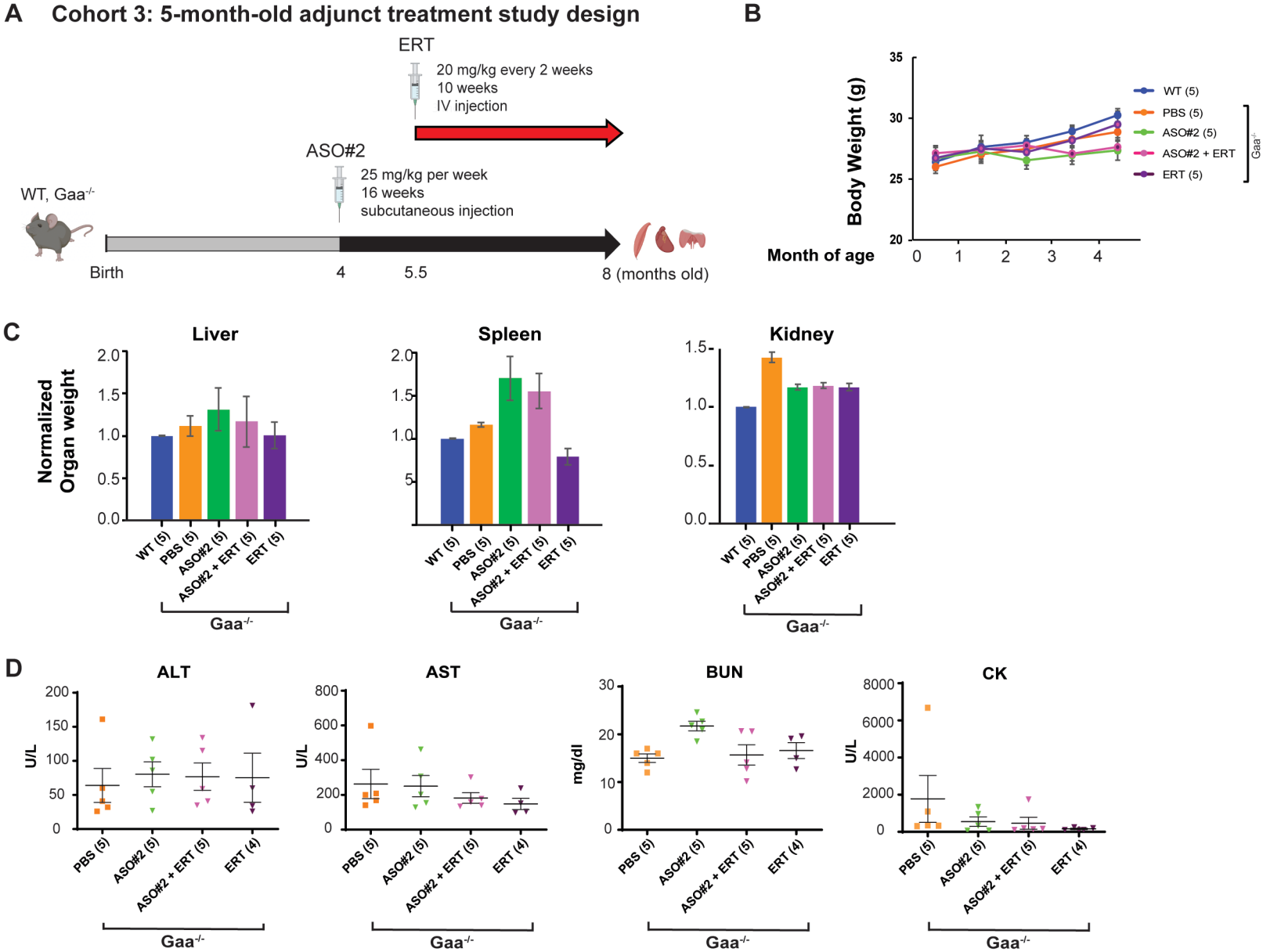
A
Cohort 3: 5-month-old adjunct treatment study design
ERT
20 mg/kg every 2 weeks
10 weeks
IV injection
ASO#2
25 mg/kg per week
16 weeks
subcutaneous injection
WT, Gaa-/-
Birth
4
5.5
8 (months old)
B
Body Weight (g)
Month of age
WT (5)
PBS (5)
ASO#2 (5)
ASO#2 + ERT
ERT (5)
Gaa-/-
C
Liver
Spleen
Kidney
Normalized Organ weight
WT (5)
PBS (5)
ASO#2 (5)
ASO#2 + ERT (5)
ERT (5)
Gaa-/-
D
ALT
AST
BUN
CK
U/L
mg/dl
PBS (5)
ASO#2 (5)
ASO#2 + ERT (5)
ERT (4)
Gaa-/-

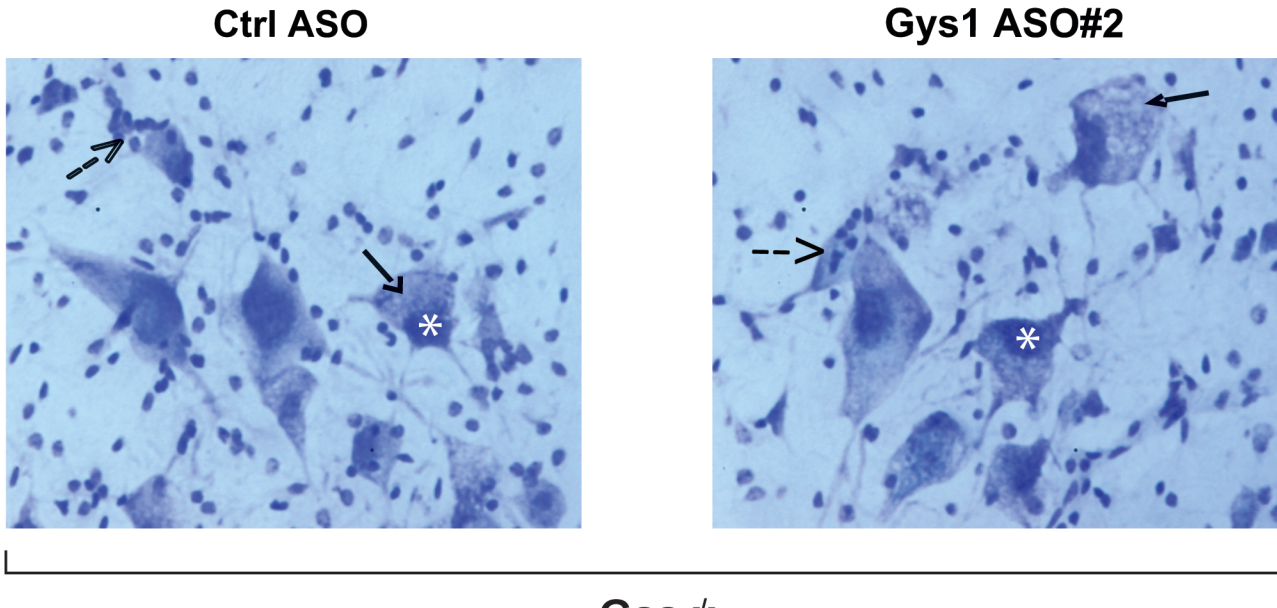
Ctrl ASO
Gys1 ASO#2
Gaa -/-